2019

Detecting Cyanobacteria Toxins: The Human Health Impact of an Environmental Problem

Lillian E. Naimie
Colby College

Detecting Cyanobacterial Toxins:
The Human Health Impact of an Environmental Problem

By Lillian E. Naimie

A Thesis Presented to the Department of Chemistry,
Colby College, Waterville, ME
In Partial Fulfillment of the Requirements for Graduation
With Honors in Chemistry

Submitted May, 2019

Detecting Cyanobacterial Toxins:
The Human Health Impact of an Environmental Problem

By Lillian E. Naimie

Approved:

_____

D. Whitney King, Dr. Frank and Theodora Miselis Professor of Chemistry

_____Date

_____

Denise Bruesewitz, Associate Professor of Environmental Studies

_____Date

Table of Contents

Vitae 3
List of Figures 4
List of Tables 6
Abstract 7
Introduction 7
Cyanobacteria 7
Toxins 7
Bloom Formation 9
Ecological Conditions 9
Microcystin 11
β-N-methylamino-L-alanine 13
Analytical Methods 16
Methods and Materials 19
Chemicals and Materials 19
MCLR ELISA Analysis 19
High-performance Liquid Chromatography 20
Mass Spectrometry Equipment 20
Results 21
HPLC/TOF MS 21
ELISA 28
Discussion 28
HPLC/TOF MS 28
ELISA 30
Conclusion and Future Directions 32
Acknowledgements 33
Appendix A: LC-MS Gradient Details 38
Apendix B: Envirologix ELISA Manual 39

Vitae

EDUCATION

Colby College, Waterville, ME — **Bachelor of Arts Expected, May 2019**
Major: Chemistry, *Concentration*: Environmental Science — **GPA 3.47**
Minor: Physics

RESEARCH POSITIONS

Colby College Chemistry Dept. Research Assistant — **Summer 2018**
Supervisor: Professor D. Whitney King
Project: Managing the internal Phosphorus load of the Belgrade lakes

Dartmouth Hitchcock Medical Center Neurology Lab Intern — **Summer 2016**
Supervisor: Elijah D. Stommel M.D.
Project: BMAA as an Environmental Risk Factor of ALS

RESEARCH PROJECTS

Honors Thesis - Quantification of Cyanotoxins on the Belgrade Lakes — **2018-19**
Advisor: Professor D. Whitney King
Credit Hours: 7

Creatine Cycling in Marine Bacterial and Phytoplankton Assemblages — **Fall 2018**
Supervisor: Deborah A. Bronk, Ph.D., President and CEO, Bigelow Laboratory

Analysis of Fluorinated Hydrocarbon Residue from Ski Wax — **2018**
Advisor: Professor D. Whitney King
Credit Hours: 4

TEACHING EXPERIENCE

Physics Teaching Assistant (Grader)
Class: Electromagnetism and Optics Grader, Professor Charles Conover — **2017-2018**
Class: Modern Physics Grader, Professor Duncan Tate — **2018**

Chemistry Lab Teaching Assistant
Class: Introductory Geo-Chemistry, Professor Karena McKinney — **Fall 2018**

Colby Outdoor Orientation Trips
Committee Member and Leader — **2016-2018**
Supervisor: Ryan Linehan

WORK EXPERIENCE

Colby College EcoRep — **2015-19**
Supervisor: Sandy Beauregard

Eastman Community Association Camp Counselor — **Summer 2017**
Supervisor: Ellen Page

SKILLS

Proficient in the use of GIS, Mathematica, Excel, Spartan, and ChemDraw

AWARDS

Colby College Analytical Chemistry Award — **2017-2018**
Colby College Office of the Provost, Special Funding Award — **Fall 2018**
Colby College Dean's List — **Spring 2016**

List of Figures

Figure 1. Photos A and B were taken on the shore of Lake Wannsee (Germany) in 2005 2, while photo C was taken by Prof. Whitney King on East Pond (2017). Both demonstrate characteristic green scum formation at the top of the water column. _____ *9*

Figure 2. The fluxes of phosphorus and nitrogen from different deposition sources (Le Moal, Gascuel-Odoux et al. 2019). _____ *10*

Figure 3. Generic structure of MC, with Z and X to denote the variable amino acid locations. _____ *11*

Figure 4. Structure of MC-LR. _____ *12*

Figure 5. The above images show, in order from left to right, a cycad tree, the seeds of a cycad, a flying fox foraging for seeds, and a stew commonly made by Chamorros, with the fruit bat fully intact. This graphic was produced by Holtcamp et al. (Holtcamp 2012). _____ *13*

Figure 6. Above is the structure of BMAA. _____ *14*

Figure 7. A graphic of the improper insertion of BMAA and its effects on protein folding, it was created by Holtcamp et al. (Holtcamp 2012). _____ *15*

Figure 8. Graphic organization of the various methods of detection for Microcystin highlighting the methods discussed in this paper are LC-MS and Immunoassay (Merel, Walker et al. 2013). _____ *17*

Figure 9. Pictorial diagram of how the ELISA kits work. Antibodies are attached to the well plate (shown in orange) which are designed to bind only with MC. Once the sample is bound, an MC-HRP conjugate is added to compete with MC for the antibody sites. After a period of competition, the amount of MC-HRP bound determines the color of the solution when a final substrate is introduced. _____ *18*

Figure 10. Shows the Total Ion Chromatograph (TIC) and Extracted Ion Chromatograph (EIC) of the first Microcystin standard run. _____ *21*

Figure 11. The full range mass spectrum at 27 minutes of the above LCTOF standard run. _____ *21*

Figure 12. Total Ion Chromatograph (TIC) and Extracted Ion Chromatograph (EIC) of a 50 ppm MCLR standard run. _____ *22*

Figure 13. Total Ion Chromatograph (TIC) and Extracted Ion Chromatograph (EIC) of a 50 ppm MCLR standard run, with the final gradient used for the rest of the method. _____ *23*

Figure 14. EIC spectrums of the triplicate runs of 50 ppm MCLR. The peak has been integrated and the peak retention time is listed above the peak. Peak integration was completed using standard peak parameters. _____ *24*

Figure 15. The triplicate MCLR serial dilutions, with a linear fit. The linear fit equation and R^2 value are displayed on the chart. _____ *25*

Figure 16. Total Ion Chromatograph (TIC) and Extracted Ion Chromatograph (EIC) of a 25 ppm BMAA standard run, with the final gradient used for the rest of the method. _____ *26*

Figure 17. The full range mass spectrum at 3.93 minutes of a BMAA standard LCTOF run. _____ *26*

Figure 18. Above are the structures of the two BMAA fragments. _____ *27*

Figure 19. The triplicate BMAA serial dilutions, with a linear fit. The linear fit equation and R^2 value are displayed on the chart. _____ *27*

Figure 20. The MCLR standards graphed with a log scale on the concentration axis and a corresponding linear fit. _____ *28*

Figure 21. The triplicate MCLR serial dilutions. The 50ppm data points are displayed, but excluded from the linear fit. The linear fit equation and R^2 value are displayed on the chart. _____ *29*

Figure 22. The MCLR standards graphed a sigmoidal fit. The two red points and corresponding doted lines pictorially demonstrate how the concentration error changes drastically over the ELISA detection range. 31

List of Tables

Table 1. The toxins produced by cyanobacteria, followed by their biochemical mode of toxicity, effect and lethal dose in mice populations. It was compiled by Dittmann et al. (Dittmann and Wiegand 2006). _____ *8*

Table 2. Lists the parameter values used for MS analysis. These parameter were optimized for electron spray ionization mass spectrometry (Barco, Rivera et al. 2002). _____ *20*

Table 3. Final gradient used for MC HPLC runs. _____ *38*

Abstract

Cyanobacteria blooms are a growing concern in the world, as they can form a dense and sometimes toxin scum on water bodies. This paper will outline and discuss the environmental conditions that produce cyanobacteria bloom with a focus on the toxins produced by blooms and specifically the detection of these toxins through two analytical methods. Of the various toxins cyanobacteria are capable of producing, this paper will focus on microcystins and BMAA, a family of hepatotoxins and a specific neurotoxin respectively. The two analytical methods discussed are liquid chromatography coupled mass spectrometry and ELISA kit techniques. The advantages and drawbacks of both methods will be compared with suggestions for future directions studying MC and BMAA in the Belgrade Lakes and elsewhere.

Introduction

Cyanobacteria

Cyanobacteria are categorized as "ubiquitous photosynthetic procariota"(Funari and Testai 2008), meaning they are found everywhere on earth, rely on light for their major energy production and lack membrane bound organelles or a nucleus. They have been found to be unicellular, colonial or multicellular, depending on the genera (Huisman, Codd et al. 2018). Additionally, they are believed to be one of the earliest organisms on Earth. They were initially termed blue-green algae due to their physical appearance on the surface of water bodies, but as a prokaryote they are truly bacteria (Dittmann and Wiegand 2006).

All families of cyanobacteria found in Maine lakes have species capable of producing toxins (commonly referred to as cyanotoxins). The bacteria families include: *Microcystis, Planktothrix, Dolichospermum, Aphanizomenon, Oscillatoria, Lyngbya, Anabaena,* and *Nodularia* genera (Le Moal, Gascuel-Odoux et al. 2019). However, four specific genera are more likely to bloom: *Microcystis, Planktothrix, Nodularia,* and *Anabaena (Barco, Rivera et al. 2002)*. Unfortunately, these four are also the most likely to produce microcystins, the most heavily researched cyanotoxin (Dittmann and Wiegand 2006). Species can be identified by microscopy, however this is a time intensive process. In recent years, the research on cyanobacteria and the toxins many are capable of producing has been consistently increasing (Merel, Walker et al. 2013). In 1985, fewer than 50 articles on the subject were published on cyanobacteria, were as in 2010 more than 1900 articles were published (Huisman, Codd et al. 2018).This rise in research is not due purely to the discovery of cyanotoxins, but also by the rise in occurrence of cyanobacteria blooms due to various environmental factors.

Toxins

Production of cyanotoxins varies between cyanobacteria strains and occurs intracellularly (Merel, Walker et al. 2013). There are three types of cyanotoxins, cyclic peptides (hepatotoxic microcystins), alkaloids (cylindrospermopsins and anatoxins), and saxitoxins (van Apeldoorn, van Egmond et al. 2007). These toxins are associated with liver, neurological, and skin damage respectively (Merel, Walker et al. 2013). The most

frequent cyanotoxins are cyclic peptides, of those Microcystin (MC) LR is the most prevalent (van Apeldoorn, van Egmond et al. 2007). Their ecological function has been the subject of intensive research (Orr and Jones 1998, Dittmann and Wiegand 2006, Ramya, Kayalvizhi et al. 2018) . Most agree that they are predominantly released during cell lysis (death) or when they experience phosphorus and nitrogen nutrient limitation (Orr and Jones 1998). When enclosed within a cell wall, the toxins lack a major pathway to the water column, so destruction of the cell wall is critical to toxin release. One previous intervention on current high biomass blooms involved treatment with algicides (copper sulphate or organic herbicides) which succeeded in lysing the cells, however it also lead to a spike in toxin level as it was released into the water (Zhang, Xie et al. 2009). The prevailing theory is that cyanobacteria produce toxic compounds specifically to kill other species of algae and bacteria and reduce P and N competition(van Apeldoorn, van Egmond et al. 2007).

Table 1. The toxins produced by cyanobacteria, followed by their biochemical mode of toxicity, effect and lethal dose in mice populations. It was compiled by Dittmann et al. (Dittmann and Wiegand 2006).

Toxin	Mode of action[a]	Main effect[a]	LD_{50} (µg/kg)[a, b]
MCs	Inhibit protein phosphatase	Liver failure and hepatic hemorrhage	25–150 (for the most toxic)
NODs	Inhibit protein phosphatase	Liver failure and hepatic hemorrhage	30–70
CYL	Inhibits protein synthesis	Liver and kidney failure	2100
ANTX-a	Binds to nicotinic acetylcholine receptors	Muscular paralysis	375
ANTX-a(s)	Inhibits acetylcholinesterase	Muscular weakness, dyspnea and convulsions	31
STXs	Bind to sodium channels	Ataxia, convulsions and paralysis	10 (for the most toxic)
BMAA	Binds to glutamate receptors	Neurodegenerative syndrome	Not specified
APTXs	Activate protein kinase C	Tumour promotion and skin irritation	Not specified
LTXs	Activate protein kinase C	Tumour promotion and skin irritation	250 (immature mice)

It is important to consider that the presence of cyanobacterial species does not definitively indicate cyanotoxin production (Sarazin, Quiblier-Llobéras et al. 2002). As stated above, all families have species which produce cyanotoxins, but those families also possess species which may not produce cyanotoxins (Le Moal, Gascuel-Odoux et al. 2019). Additionally the presence of strains capable of producing cyanotoxins does not

definitively indicate the presence of those toxins(Huisman, Codd et al. 2018). It is essential to consider the words of Paracelsus before taking drastic action against cyanobacteria. “All things are poison and nothing is without poison; only the dose makes a thing not a poison.” It cannot be said that human health is in danger purely because we can detect a substance known to be toxic. All aspects must be properly placed in context, before we can draw conclusions, or determine steps of intervention. This will require analysis of cyanotoxin concentration in the water column, and contained intracellularly.

Bloom Formation

A cyanobacteria bloom occurs when there is a significant production of cyanobacterial biomass, built up in a short period of time, and a decrease in the biodiversity of phytoplankton(Merel, Walker et al. 2013). They are frequently marked by a foul odor and formation of a green scum on the surface of the water source. The scum layer on the top of the water column is due to movement of cyanobacteria upwards in the water column via gas vesicles in the cyanobacteria: small intentional bubbles to create buoyancy. These bubbles allow them to float up where they have access to light, and out compete other phytoplankton (Dittmann and Wiegand 2006). In regards to cyanotoxins, the biodiversity of bacteria in the bloom impacts their production. Toxin production is highest when the population contains only a few different species of cyanos (Sarazin, Quiblier-Llobéras et al. 2002). Thus, direct measurement of cyanotoxin concentration is required to determine toxin production even during a bloom.

Figure 1. Photos A and B were taken on the shore of Lake Wannsee (Germany) in 2005 2, while photo C was taken by Prof. Whitney King on East Pond (2017). Both demonstrate characteristic green scum formation at the top of the water column.

Bloom severity is often measured by Chlorophyll a concentration or Secchi depth, however the first does not differentiate between cyanobacteria and algae, and the latter measures water column transparency (Merel, Walker et al. 2013). Measurement of phycocyanin (a pigment produced by cyanobacteria) could be taken, however this again would only approximate the bloom size and not the toxin production.

Ecological Conditions

Blooms tend to form when lakes are eutrophic because phosphorus and nitrogen are essential for algae growth and the high concentration of these nutrients, as seen in eutrophication, promotes the rapid cell division which characterizes “blooming” (Merel, Walker et al. 2013). Increased temperature, higher light exposure, stable water columns, and longer residence time of water bodies has also been shown to impact bloom formation (Atia and Saad 2014). The eventual decomposition of a bloom will consume

oxygen at the bottom of the water column, increasing the risk of anoxic zones in the lake or areas completely lacking oxygen (Le Moal, Gascuel-Odoux et al. 2019). This depletion of oxygen puts the deep water fish, species which typically require high levels of oxygen, at risk when the lake has formed a thermocline. This thermocline will prevent top to bottom mixing of the lake, so although colder water dissolves more oxygen, as it gets depleted by the bacteria growth it will not be replenished until the lake mixes. Anoxia amplifies the blooms by driving internal phosphorus and ammonium loading from the sediments to the water column (Le Moal, Gascuel-Odoux et al. 2019).

Blooming has a world-wide impact due to its pervasiveness: affecting freshwater lakes, estuaries, ground water and rivers (Le Moal, Gascuel-Odoux et al. 2019). The addition of nutrients (phosphorus and nitrogen) to global waterways has doubled in the 20th century (Beusen, Bouwman et al. 2016). Nutrient collection and distribution to other waterbodies and their respective base sediments by ground water has also increased, but not by a sufficient amount to counteract the increase in loading (Beusen, Bouwman et al. 2016). This dramatic increase can be directly linked to increasing populations, urbanization, and industrialization of agriculture (Le Moal, Gascuel-Odoux et al. 2019). Due to ground water distribution of P and N, inputs from up to a thousand kilometers away could be impacting a given site(Pinay, Peiffer et al. 2015). This increasing eutrophication leads to manifestation of cyanobacteria blooms in freshwater and build-up of green macro-algae in salt water environments (Le Moal, Gascuel-Odoux et al. 2019). Due to their inclination for warm water, it has also been indicated that the occurrence of blooms will only increase as the average temperature of the Earth increases (Paerl and Huisman 2008).

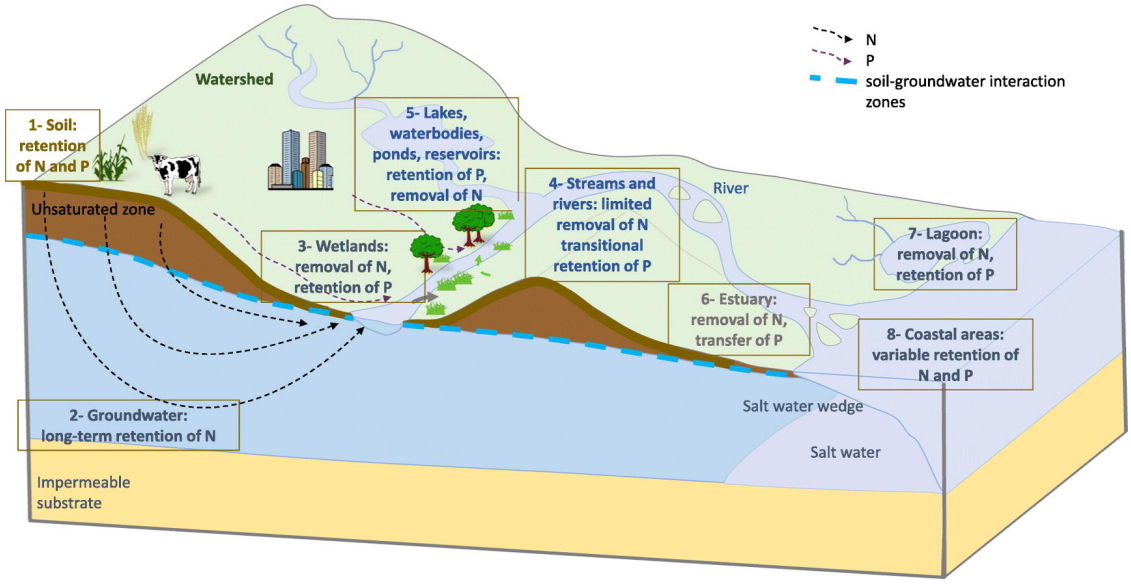

Figure 2. The fluxes of phosphorus and nitrogen from different deposition sources (Le Moal, Gascuel-Odoux et al. 2019).

Programs like LakeSmart("LakeSmart"), which encourages home owners to contribute to protecting the lake near them, could be effective at decreasing lake eutrophication. Reduction in phosphorus and nitrogen pollution sources has been shown

to have an effect on the number instances of eutrophication (Le Moal, Gascuel-Odoux et al. 2019). Specifically at Lake Erie (United States) and Lake Geneva (France-Swiss), the ban on phosphates in detergent and improved sewage systems have had positive, but gradual effects (Le Moal, Gascuel-Odoux et al. 2019).

In Maine, increasing temperature in the summer makes blooms most prominent in late summer or early fall (van Apeldoorn, van Egmond et al. 2007). Lake stability increases due to the summer stratification, and as discussed above, warmer water temperatures increases the likely hood of a bloom event. The nutrient pattern of the lake is also distinct in this time period. At the beginning of the summer there is a higher stoichiometric ratio of dissolved nitrogen and phosphorus, thus algae species requiring nitrogen make up most of the bloom. Towards the end of the summer nitrogen is limited, which allows cyanobacteria capable of fixing gaseous nitrogen to out compete species that cannot (van Apeldoorn, van Egmond et al. 2007). Although not all cyanobacteria are capable of fixing nitrogen from the atmosphere, many are, giving them a competitive advantage.

Microcystin

For the purposes of this project, we will attempt to measure the concentration of two groups of cyanotoxins: Microcystins (MC) and β-N-methylamino-L-alanine (BMAA). The first, microcystins, are cyclic heptapeptides containing seven amino acids. The structure varies based on the insertion of different amino acids in the ring, creating more than 80 isoforms (Dittmann and Wiegand 2006). These are mostly within 900-1100 Daltons (van Apeldoorn, van Egmond et al. 2007), with the most common and most toxic being MC-LR (van Apeldoorn, van Egmond et al. 2007). MC-LR has leucine and arginine at the Z and X cites respectively (Dawson 1998) as is shown below.

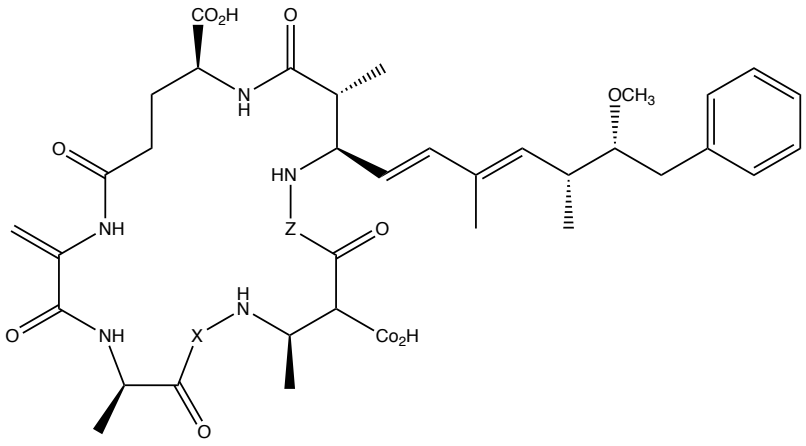

Figure 3. Generic structure of MC, with Z and X to denote the variable amino acid locations.

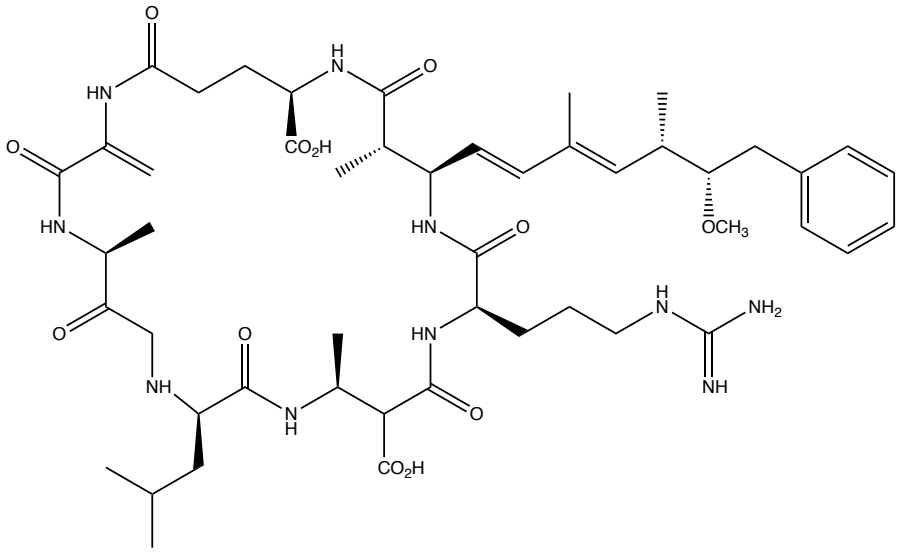

Chemical Formula: $C_{49}H_{74}N_{10}O_{12}$
Exact Mass: 994.55
Molecular Weight: 995.19
m/z: 994.55 (100.0%), 995.55 (53.0%), 996.56 (13.8%), 995.55 (3.7%), 996.55 (2.5%), 996.55 (2.0%), 997.56 (1.5%), 997.56 (1.3%)
Elemental Analysis: C, 59.14; H, 7.50; N, 14.07; O, 19.29

Figure 4. Structure of MC-LR.

Understanding the structure of MC and its different isoforms is essential to understanding their toxicity. The branch present in both figures, terminating with a benzene ring, is an Adda amino acid called the Adda region (van Apeldoorn, van Egmond et al. 2007). Adda is an extremely rare amino acid, whose toxic properties come from the conjugated diene located in the middle (Dawson 1998). Changes to the Adda region lead to a reduction in toxicity (van Apeldoorn, van Egmond et al. 2007). There are six enzymes responsible for the biosynthesis of MC, all of which are coded for by the MCY gene cluster. These enzymes are either nonribosomal peptide synthetases (NRPS) or polyketide synthases (PKS-I) (Dittmann and Wiegand 2006). Similar enzymes found in many prokaryotes and lower eukaryotes produce antibiotics, antifungals and other diverse compounds (Dittmann and Wiegand 2006). It has also been demonstrated that the half-life of MCs in the water column is 4-14 days (EPA 2016).

The method of toxicity in mammals is well established for microcystins. Firstly, they accumulate in the liver after ingestion and act as a hepatotoxin (Dittmann and Wiegand 2006). The tendency to accumulate in the liver was well established by Robinson et al. in a mouse model, where they administered radioactively labeled MC and determined that more than half of it went to the liver (Robinson, Pace et al. 1991). Inside the liver, MCs are shown to cause "rapid, irreversible, and severe damage to the liver"(Dawson 1998). They accomplish this by inhibiting protein serine and threonine phosphatases (PP1 and PP2A) (Dittmann and Wiegand 2006), which leads to a protein phosphorylation imbalance. This imbalance damages the liver cytoskeleton and causes hemorrhage and cell death, colloquially known as liver failure (Dawson 1998). The inhibition of PP1 and PP2A have K_i (inhibition constant) values of less than 0.1nM (MacKintosh, Beattie et al. 1990). The inhibition constant is a measure of how strongly the inhibitor binds to an enzyme, the low value given indicates that MCs bind strongly to PP1 and PP2, thus inhibiting strongly. It should be noted that while the liver experiences

most of the protein phosphorylation related damage, the mechanism of toxicity is the same for all mammalian cells (Dittmann and Wiegand 2006). Conversely, Cyanobacterial protein phosphatases are insensitive to inhibition PP1 and PP2A caused by MC (Shi, Carmichael et al. 1999). MCs also have two other mechanisms of toxicity: they stimulate preneoplastic cells (tumors) in the liver, and lead to the formation of ROS species, which cause cellular oxidative damage (Dittmann and Wiegand 2006).

β-N-methylamino-L-alanine

The second molecule of interest, β-N-methylamino-L-alanine (BMAA), does not have the high number of isoforms seen with MC, however as a more newly discovered cyanotoxin there is less available research but see (Lobner, Piana et al. 2007, Holtcamp 2012). The neurotoxicity of BMAA was first suggest in 1967, where preliminary research showed it to cause convulsions in chicks and rats (Holtcamp 2012). It was theorized that its presence in cycads (commonly used to make flour in Guam) was causing the unthinkably high rate of a neurodegenerative illness in the Chamorros, the indigenous peoples of Guam. They were experiencing AL-SPDC, a neurodegenerative disease with many of the same symptoms as ALS, Parkinson's, and Alzheimer's, at 50-100 times the expected rate (Bradley and Mash 2009). BMAA is produced due to a symbiotic relationship between cyanobacteria and cycad trees, where cyanobacteria colonies populate the roots of the cycad trees (Cox, Banack et al. 2003). Its presence is then biomagnified up the food chain as flying foxes eat them cycad seeds. These fruit bats are prized game in Guam, and are often stewed and eaten whole (Holtcamp 2012). This accumulation of BMAA in the food system is believed to be behind the occurrence of ALS and PDC found in Guam.

Figure 5. The above images show, in order from left to right, a cycad tree, the seeds of a cycad, a flying fox foraging for seeds, and a stew commonly made by Chamorros, with the fruit bat fully intact. This graphic was produced by Holtcamp et al. (Holtcamp 2012).

On average, a brain concentration of 627μg/g protein bound BMAA, was found in Chamorros dying from ALS/PDC, but not in controls (Bradley and Mash 2009). Further study found BMAA in the brains of patients with ALS, Parkinson's and Alzheimer's in North America, with an average concentration of 268μg/g, but in the brains of patients with Huntington's disease only an average of 11μg/g (Banack, Caller et al. 2010). The lack of evidence in patients with Huntington's disease is significant, the development of Huntington's is hereditary, so this data suggests that the development of ALS, Parkinson's and Alzheimer's may differ fundamentally. This has lead increasing research to be conducted on non-genetic pathways of development. Clusters of ALS occurrence have also been seen by Stommel et al. 2015 surrounding lakes known to produce cyanobacterial blooms in Western New Hampshire (Banack, Caller et al. 2010). Around Lake Mascoma specifically, the rate of incidence is 10-25 times the expected, indicating BMAA may be an environmental risk factor for ALS (Caller, Doolin et al. 2009).

The leading current theory is that BMAA, released by cyanobacteria acts as a neurotoxin, and is an environmental risk factor for neurodegenerative development. Many recent studies hypothesize that people who develop severe neurodegeneration have a complex interplay of environmental factors such as BMAA and genetic predisposition(Bradley and Mash 2009). Ninty-five percent of cyanobacteria species tested produced BMAA(Cox, Banack et al. 2005). In order to understand the neurotoxic effects of BMAA, we must understand its chemical structure, and pathway of toxicity. BMAA is a non-protein amino acid(Cox, Banack et al. 2005), meaning it is not one of the primary amino acids which make up proteins in eukaryotes.

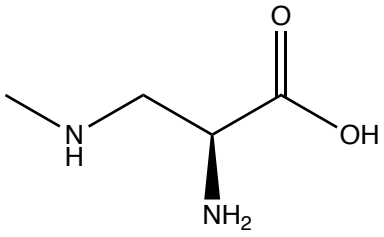

Chemical Formula: $C_4H_{10}N_2O_2$
Exact Mass: 118.07
Molecular Weight: 118.14
m/z: 118.07 (100.0%), 119.08 (4.3%)
Elemental Analysis: C, 40.67; H, 8.53; N, 23.71; O, 27.09

Figure 6. Above is the structure of BMAA.

The presence of two structural isomers: N-2-aminoethylglycine (AEG) and 2,4-diaminobutyric acid (2,4DAB)(Beri, Kirkwood et al. 2018) pose an additional challenge when analyzing BMAA. Initial analysis found only an average concentration of 6.6μg/g (Cox, Banack et al. 2003), in Chamorro brains, when the tissue was hydrolyzed to release protein-bound BMAA however, that value increased to 627μg/g(Bradley and Mash 2009) as reported above. This more than 80-fold increase is the basis for the theory of the current mechanism of toxicity. BMAA is sometimes erroneously inserted into proteins, in place of the amino acid serine, which causes the protein chain to fold improperly(Murch, Cox et al. 2004). These improperly folded proteins can aggregate, and cause cell death(Caller, Henegan et al. 2018).

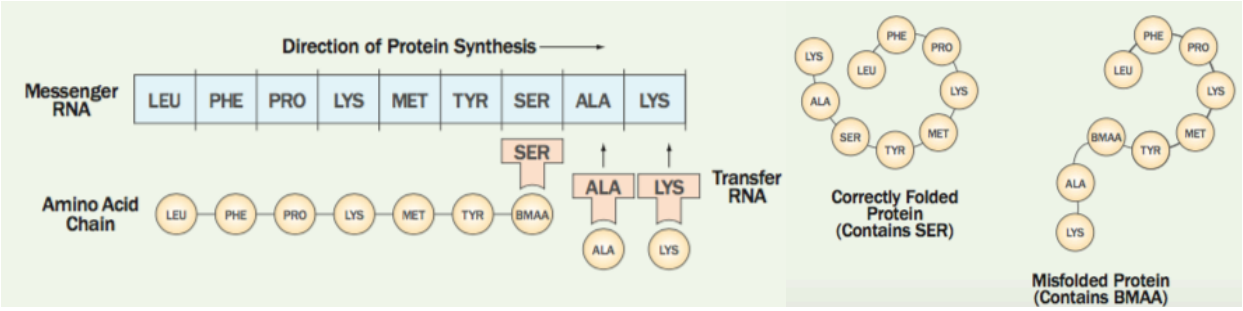

Figure 7. A graphic of the improper insertion of BMAA and its effects on protein folding, it was created by Holtcamp et al. (Holtcamp 2012).

The way that BMAA is bound in protein is not the main mechanism of neurotoxicity, the binding predominantly explains the delayed onset of symptoms due to slow release in the body (Murch, Cox et al. 2004). Accumulation leads to misfolding proteins, toxic in their own right and additional toxic effects when they are released. Early experiments showed acute toxicity, when animal models were exposed to extremely high amounts, however one of the main problems with this was that it does not explain the delayed onset of ALS/PDC(Caller, Henegan et al. 2018). In terms of neurotoxicity specifically, BMAA is believed to target motor neurons in the brain. Motor neurons are the "largest and longest living cells in the body", thus making them at risk for accumulated damage (Banack, Caller et al. 2010). This neurodegeneration encompasses three distinct factors: it is an agonist for NDMA and mGLuR5, and enhances oxidative stress(Lobner, Piana et al. 2007). Even a concentration of as low as 10 μM can potentially cause neurological affects (Lobner, Piana et al. 2007). Their data suggests that over long periods of exposure, BMAA could lead to profound neuronal death. Binding to the glutamate receptors both NDMA and mGLuR5, induces depolarization and changes the internal cellular calcium concentration(Caller, Henegan et al. 2018), this increased calcium concentration is detrimental to the cell and can lead to cell death. Oxidative stress, is because BMAA reduces the amount of glutathione in the cell, which has a protective affect against ROS species (de Munck, Munoz-Saez et al. 2013). Activity of NDMA is essential for neuron function, and disruption of function has been linked to most neurodegenerative diseases (including PDC) (Lipton 2004), while malfunction in mGLuR5 has been linked to mainly Parkinson's (Marino, Valenti et al. 2003).

For the purposes of this paper, we will consider cyanotoxin exposure associated exclusively with bloom formation and people living around blooming lakes. Exposure routes include: consuming contaminated lake water, swimming in bacterial blooms (skin contact, inhalation, accidental drinking), consumption of bio accumulators (fish, shellfish etc.) and inhalation of aerosolized particles (Dittmann and Wiegand 2006). BMAA has also been found at relatively high concentrations in fish species living in the New Hampshire lakes which experience ALS clustering. This has also been supported by data from other water bodies with cyanobacteria blooms, including Lake Michigan (United States), and Thau Lagoon (France)(Banack, Caller et al. 2015). However due to the low numbers of individuals eating these fish in Maine, this is most likely not a major exposure pathway. Aerosolization has been demonstrated soundly for MCs (Stommel, Field et al. 2013), and new research shows detectable aerosolization of BMAA particles, surrounding New Hampshire lakes (Banack, Caller et al. 2015). This aerosolization occurs from waves on the lake, water vapor formation due to temperature changes,

impact of precipitation (Stommel, Field et al. 2013), and the bursting of gaseous bubbles released by cyanobacteria during photosynthesis, when they reach the air-water interface (Yung, Zhou et al. 2007). There is not robust enough data on quantity aerosolized to quantity ingested and accumulated for BMAA, to accurately determine what water concentration would put a population living around the lake in imminent danger (Rodgers, Main et al. 2018).

With MCs we are better able to predict an unsafe water concentration level, because they are acutely toxic and there has been more robust research over the years (Barco, Rivera et al. 2002, Dittmann and Wiegand 2006, Fontanillo and Köhn 2018). (Atia and Saad 2014)The Maine Department of Environmental Protection sets the guideline for recreational water based only on Secchi depth, and the guideline for dangerous blooming at a Secchi of less than two meters(EPA 2016). For reasons discussed above in the paper however, Secchi is an ineffective measure of toxicity. The WHO (World Health Organization) has set the safety limit for drinking water at 1 μg/L MC ((Dittmann and Wiegand 2006) MCs. The WHO value was created from data collected during a mouse study by Fawell et al. in 1999(Fawell, Mitchell et al. 1999). Dittmann suggests however that because the WHO failed to incorporate the tumor promoting capacity of MCs, and that this guideline should be increased by a factor of three(Dittmann and Wiegand 2006) (to 3 μg/L). The higher number suggested by Dittmann is also the published US Environmental Protection Agency value. For recreational water, their guideline is a higher at 2 ppb (EPA 2016). The WHO publishes the there is a risk of adverse effects from 2-4 ppb Microcystin, moderate risk of health effects at 20 ppb and high risk of health effects above 100 ppb.

Analytical Methods

With these standards in mind, it is crucial to develop detection methods which will encompass the range of values used to determine the threat to public health and establish regulatory limits. The limits published by the WHO and other sources should be used by future work to determine risk of toxicity after quantification of BMAA and Microcystin. The methods can generally be separated into the following categories: those which require assays to select for specific molecules and chromatographic techniques, which rely on the separation of compounds due to their chemical properties. Generally speaking the assay based techniques are much more affordable, however they have higher limits of detection when compared with techniques involving mass spectrometry (Merel, Walker et al. 2013).

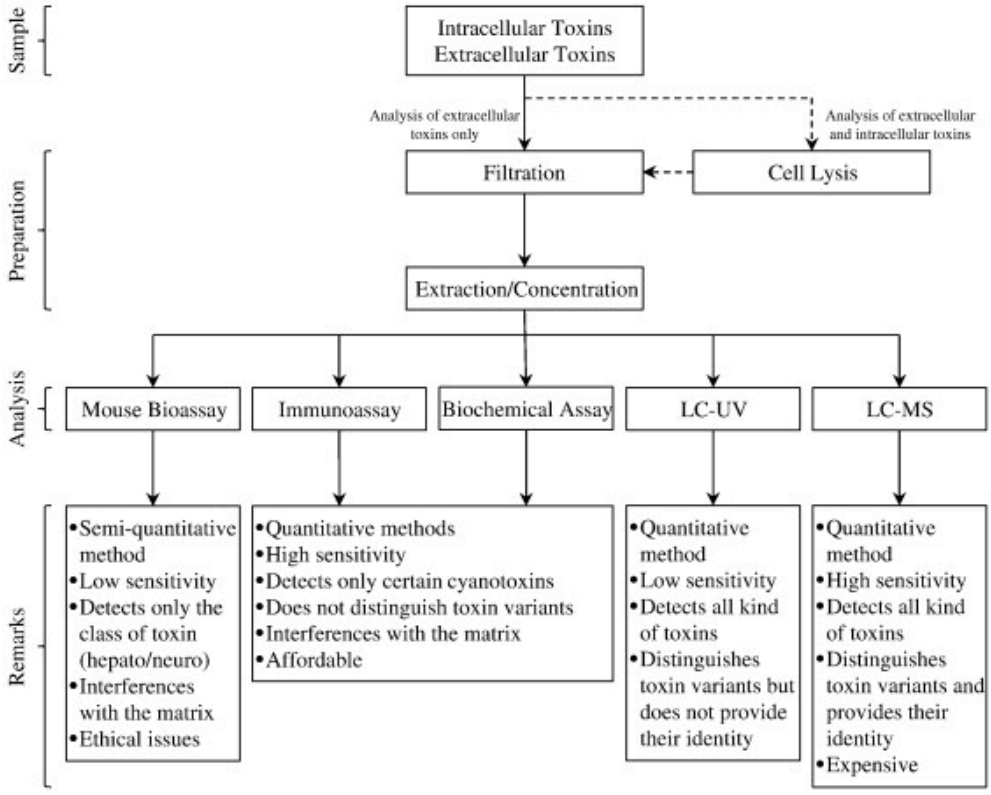

Figure 8. Graphic organization of the various methods of detection for Microcystin highlighting the methods discussed in this paper are LC-MS and Immunoassay (Merel, Walker et al. 2013).

Filtration and extraction are key steps in the analysis of either of these compounds, because they are present at low concentration in samples and there are many other compounds in the samples. The presence of a diverse array of other compounds requires steps to select for those which are desired. A common technique for extraction is using an SPE (Phase selection) C_{18} cartridge, which retains hydrophobic compounds and then allows them to be eluted off using a different solvent (Botes, Kruger et al. 1982). Some papers focus on extracting toxins without breaking the cell wall, however because the cells must eventually lyse and release those toxins, it is not important to avoid this cell breakdown initially. As data collection progresses it will be important to include cell lysing techniques, or take additional measurements as the blooms die to determine the maximum water column concentration. Due to its low sensitivity and access to MS techniques, this paper will also not consider chromatographic techniques using UV as a detection source. Therefore, we are left to compare mass Spec and assay techniques.

Assay techniques can be broken down into biochemical and immunoassay techniques. Biochemical assays detect the amount of certain cellular processes, so measure the amount of MC or BMAA based on the specific inhibition associated with those compounds. This technique has been successfully used for Microcystin (Ma, Li et al. 2018), however is not commercially available. Immunoassay techniques rely on specific antibodies to bind to the desired chemical compound. The most common immunoassay for Microcystin (Merel, Walker et al. 2013) is ELISA (Enzyme-Linked ImmunoSorbent Assay). These systems are commercially available and produce a color change when the target compound binds with the antibodies. They are similar to other

immunoassay labeling systems, such as radioactivity, however they use a specific enzyme to chemically label a compound of choice (Lequin 2005). ELISA measures absorbance as the antibody bound compound is introduced to a different substrate. One issue is that most ELISA systems for Microcystin cannot distinguish between different MC variations, and they report the concentration of the most toxic form, MC-LR (Merel, Walker et al. 2013). This is an issue because the different isoforms have different levels of toxicity, and MC-LR is the most toxic, indicating that these systems may overestimate the risk associated with a given concentration of MC.

The kit that used for this project was a competitive ELISA kit, while many companies have developed kits, this project utilized a kit purchased from Envirologix (Portland, ME).

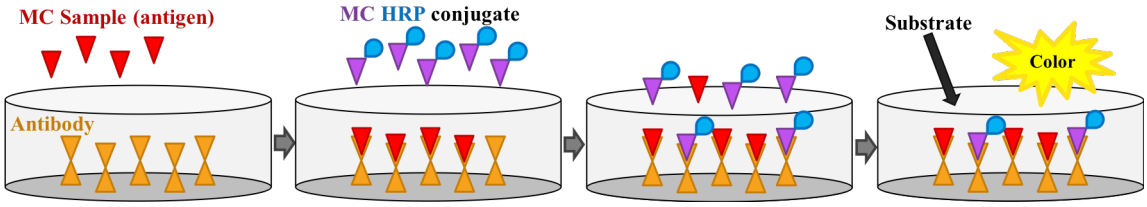

Figure 9. Pictorial diagram of how the ELISA kits work. Antibodies are attached to the well plate (shown in orange) which are designed to bind only with MC. Once the sample is bound, an MC-HRP conjugate is added to compete with MC for the antibody sites. After a period of competition, the amount of MC-HRP bound determines the color of the solution when a final substrate is introduced.

Each well of the kit has a population of antibodies on the base, which are designed to bind with the antigen. For this project that antigen is Microcystin. The first step is to add a sample to the well, then the molecules of antigen will bind to the antibody. Excess sample is flushed away, and a pre-made Microcystin-HRP (horse radish peroxidase) conjugate is added to fill the empty antibody sites. Additionally, the MC-HRP will compete with the sites that already have a Microcystin bound, and some exchange will occur. After a set amount of time this solution is washed away and a substrate is added which when catalyzed by HRP undergoes a chemical reaction changing its color. This color change is easily measured using the SpectraMax Microplate reader. Known solutions give a calibration curve that relates sample concentration to absorbance, which can be used to calculate the concentration of unknown samples. The detection range of this Envirologix kit is 0.2 to 2 ppb. The upper range is the recreational limit as given by the WHO. When concentrations exceed 2 ppb we will not have an accurate concentration. For samples that exceed 2 ppb we will either need to dilute the samples or rely on other techniques to determine the exact concentration.

Mass spectrometry (MS) techniques are the last of those generally used to detect these cyanotoxins. MS techniques have a much higher associated cost, and are not portable, but they provide a more sensitive detection of both BMAA and Microcystin. Another advantage for these techniques for our project is that Colby already has the necessary instruments, and thus there is only a small amount of additional cost associated with running samples. MCs are too large and easily fragmented to attempt GC (Gas Chromatography). CZE/MS (Capillary Zone Electrophoresis) has also been used to identify BMAA(Beri, Kirkwood et al. 2018). CZE/MS operates under a similar principle as LC, where different compound migrate through a capillary (in LC this would be the column) with different velocities based on their chemical properties(Chasteen 2003,

2005, 2006). The presence of structural isomers of BMAA presents a challenge, but because their retention times are all slightly different we should be able to differentiate between them.

Solid Phase Extraction can be used to concentrate lake water samples during bloom events, with the suggested C_{18} solid phase. Then MC and BMAA will be identified and quantified using LC/TOF MS (Liquid Chromatography Time of Flight Mass Spectrometry). The liquid chromatography will be conducted with a Zorbax 300 C_{18} column from Agilent Technologies. Samples will be eluted in acetonitrile and water, both prepared at 0.01% (v/v) trifluoroacetic acid. TFA is added as an ion pairing agent, to improve the ionization efficiency of the method. The TOF will be run in positive ion mode due to the presence of easily ionizable nitrogen in both compounds. The detection will be run over a mass range of 20 to 1500 m/z in continuous ion mode. A large benefit of LC/TOF MS at Colby is the accompanying autosampler, allowing for multiple samples to be run by the instrument. The quantification will be based on comparison to known standards, which will be purchased from Thermo Fisher Scientific. These will create a calibration curve and act as an internal standard to improve our sensitivity.

Developing and comparing analytical methods of MC and BMAA concentrations will allow future researchers to collect reliable and accurate data on cyanotoxins produced by blooms in the Belgrade Lakes. Specifically, this work will seek to compare the advantages and disadvantages of HPLC/MS methods and ELISA methods. It will seek to find a method with low detection limits, with efficient sample processing that is also cost effective.

Methods and Materials

Chemicals and Materials

All solvents, except isopropanol, were purchased at high-performance liquid chromatographic (HPLC) or ultra-high-performance liquid chromatographic grade (UHPLC). The isopropanol was used exclusively for cleaning, and was purchased at analytic grade. Acetonitrile, methanol, trifluoroacetic acid and isopropanol were purchased from Fisher Scientific (Friendship, ME).

Microcystin-LR (MCLR) standard was purchased from Fisher Scientific (Friendship, ME). Beta-Methylamino-L-Alanine (BMAA) was purchased from Sigma-Aldrich (Burlington, MA). The MCLR analyte was prepared at a concentration of 50 ppm in 70% methanol and stored at 4°C. The BMAA analyte was prepared at a concentration of 500 ppm in MilliQ water and stored at 4°C.

MCLR ELISA Analysis

The EP-022 ELISA kit was purchased from Envirologix (Portland, ME; Figure 9). This is the base range Microcystin-LR kit and rated to detect from 0.2-2 ppb concentrations in water samples. The procedure was conducted following the Envirologix ELISA kit manual (2018). The full Envirologix MC ELISA manual can be found in Apendix B, this includes operating procedure and data analysis instructions. The plates were run on a M5 SpectraMax Absorbance plate reader. Absorbance measurements were taken at 450 and

630 nm. The standards with the kit were run in triplicate. Data analysis was performed in accordance with manufacturer specifications.

High-performance Liquid Chromatography

Gradients and polarity were explored in terms of the length and strength of the gradient to maximize resolution while minimizing analytical time. MilliQ water and HPLC grade Acetonitrile were used for these extractions. Both solvents were prepared at 0.01% (v/v) trifluoroacetic acid. The liquid chromatography components of the system were composed of a 1260 infinity binary pump, and autosampler from Agilent Technologies. The column used was an Agilent Technologies Zorbax 300 C_{18} column, 2.1 mm by 150 mm, with an internal diameter of 3.5 μm. The flow rate for all samples was set to 0.2 ml/min with an injection volume of 5 μL. The run time for each sample was 25 minutes. A calibration curve was made by running triplicates of serial dilutions of a MCLR standard.

Mass Spectrometry Equipment

Mass spectrometry measurements were taken on the 6230 time of flight (TOF) instrument (Agilent, Santa Clara, CA). Toxins were analyzed in positive ion mode. Nitrogen was used as a drying gas. The mass spectrometer was run in continuous ion mode at 10 spectra/s, over a full-scan mass spectra range of 20 to 1500 m/z for MCLR and over a smaller range (20 to 500 m/z) for BMAA. BMAA has such a smaller mass that it did not require the full mass scan used for MCLR. The parameters for MS analysis are given in the table below.

Table 2. Lists the parameter values used for MS analysis. These parameter were optimized for electron spray ionization mass spectrometry (Barco, Rivera et al. 2002).

Parameter	**Value**
Capillary voltage	3250 V
Cone voltage	50 V
Skimmer	1.6 V
Skimmer lens offset	5.0 V
RF lens	0.2 V
Ion energy	1.1 V
Mobile phase flow rate	0.200 ml/min
Gas flow rate	15 ml/min
Source temperature	150 °C

Results

HPLC/TOF MS

Using the MS parameters in Table 2 and a solvent gradient from XXX to YYY over ZZZ minutes produced acceptable separation of MCLR (Figure 10).

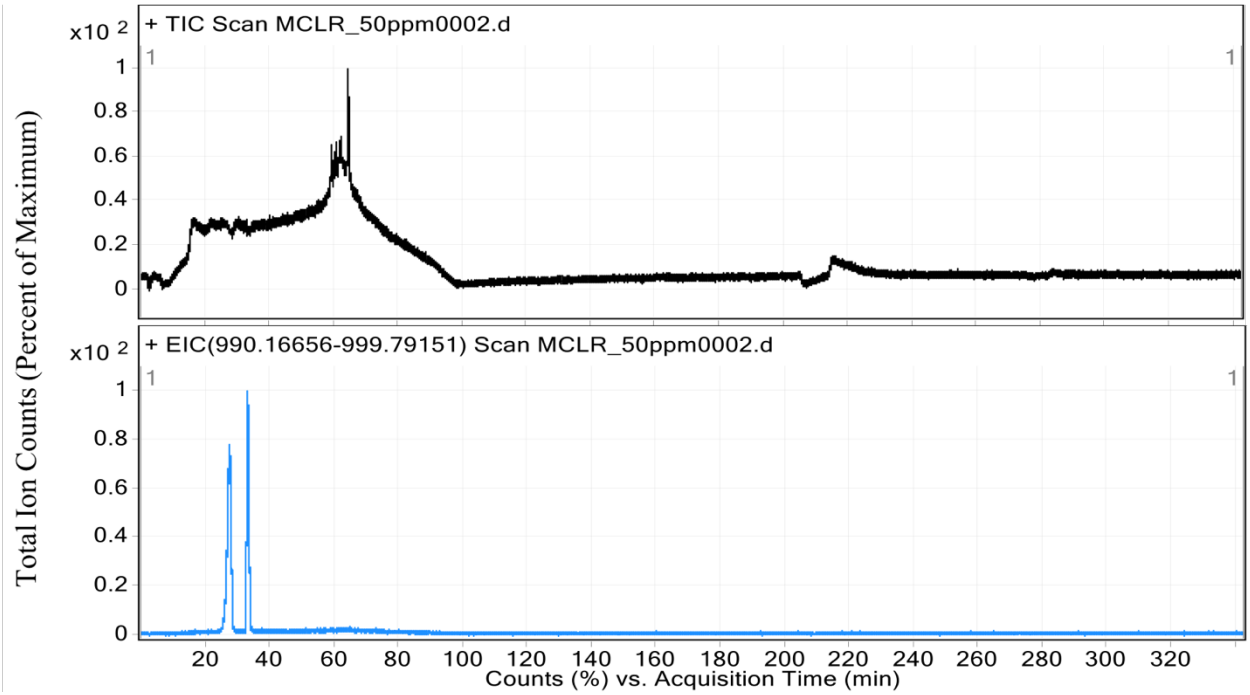

Figure 10. Shows the Total Ion Chromatograph (TIC) and Extracted Ion Chromatograph (EIC) of the first Microcystin standard run.

The TIC was extracted over a range of 990.20 – 999.79 m/z to encompass the expected mass of MCLR, 995.55 amu. This mass is as given in Figure 4, plus one due to the positive ion being created for this method. Over this mass range two distinct, base line resolved peaks appear with retentions times of 27 and 33 minutes. The mass spectrums of these peaks were then analyzed to confirm they are MCLR.

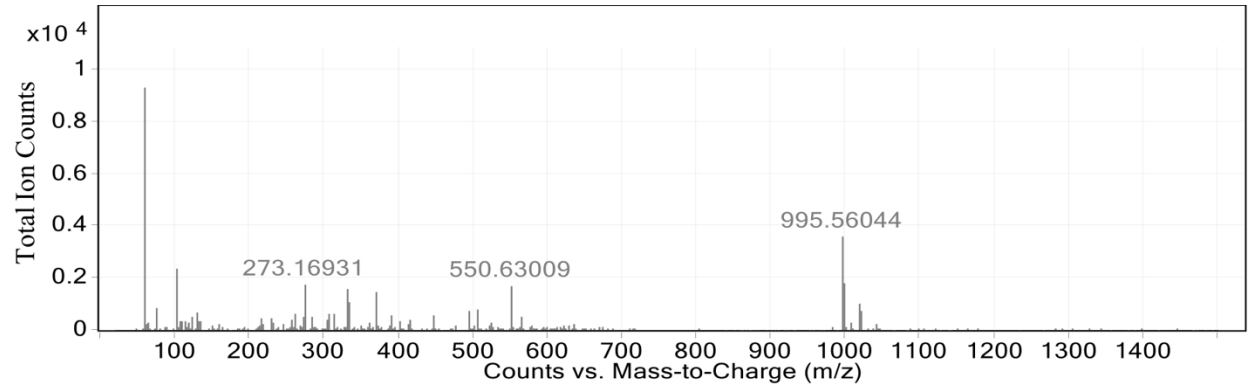

Figure 11. The full range mass spectrum at 27 minutes of the above LCTOF standard run.

The above mass spectrum has a clear parent mass peak at 995.56044 m/z, matching our desired mass peak. Analyzing the isotope ratios further indicates this is the mass spectrum of MCLR. From Figure 4, the expected (+1) isotope ratio is 53% and the expected (+2) isotope ratio is 13%. In the above mass spectrum the calculated ratios are 53.9% and 12% respectively. The mass spectrum was used to confirm the identity of MCLR for each subsequent run.

The solvent gradient was then manipulated to achieve a shorter retention time, and overlap of those two distinct peaks. This involved running more than 40 distinct gradients, an example of which is shown below.

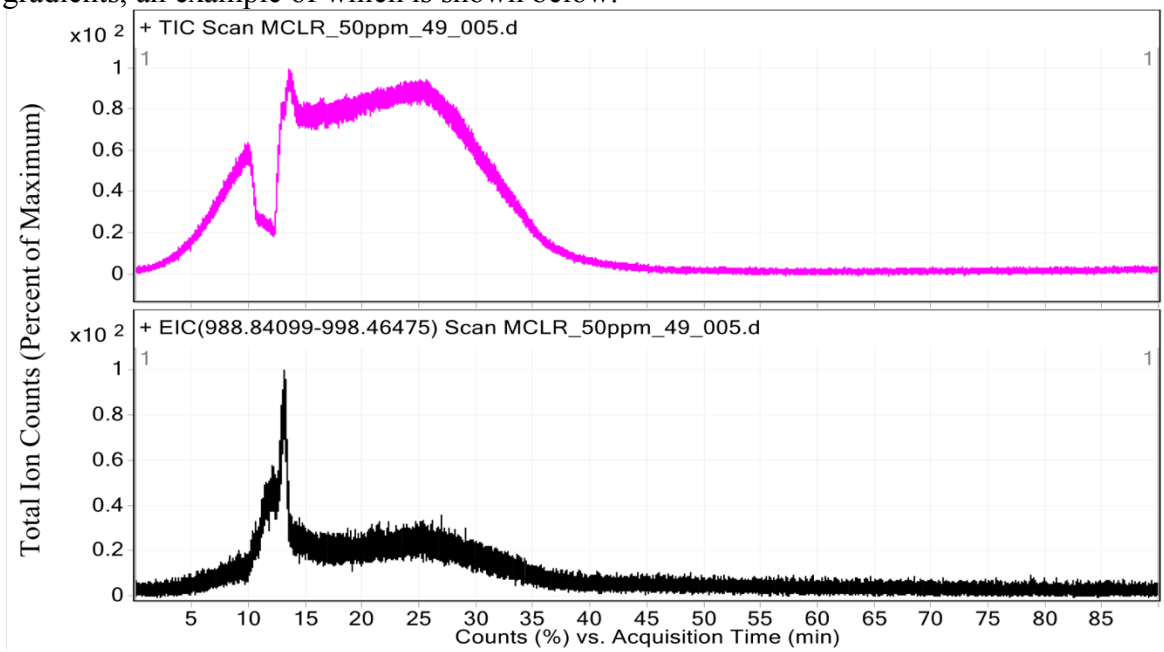

Figure 12. Total Ion Chromatograph (TIC) and Extracted Ion Chromatograph (EIC) of a 50 ppm MCLR standard run.

The graphs in Figure 12 show a new gradient with a MCLR retention time of 14 minutes. This gradient still has an extremely slow ramp down phase and lasts 90 minutes. After many gradient attempts a final gradient was selected.

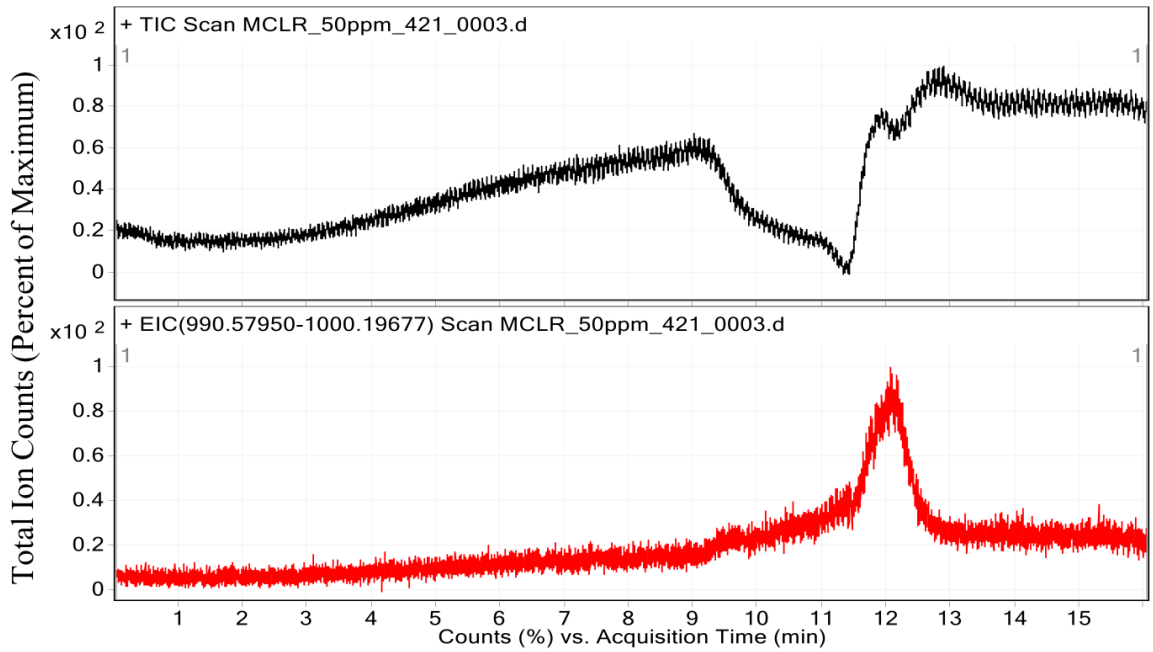

Figure 13. Total Ion Chromatograph (TIC) and Extracted Ion Chromatograph (EIC) of a 50 ppm MCLR standard run, with the final gradient used for the rest of the method.

The final gradient selected had a 12.7 minute retention time, and took 25 minutes for a complete run. The end of the run is not shown in Figure 13 to highlight the MCLR peak and retention time. The EIC in Figure 13 show a singular MCLR peak which can be easily integrated. Details of the gradient are provided in Appendix A.

Serial dilutions were then prepared to create a calibration curve. Each concentration was run with the same method, in triplicate on the instrument. The dilution values ranged from 10 to 50 ppm. The calibration curve compared known concentration to the integrated peak area of the EIC spectrum. An example of the extracted and integrated EIC sample runs are shown below.

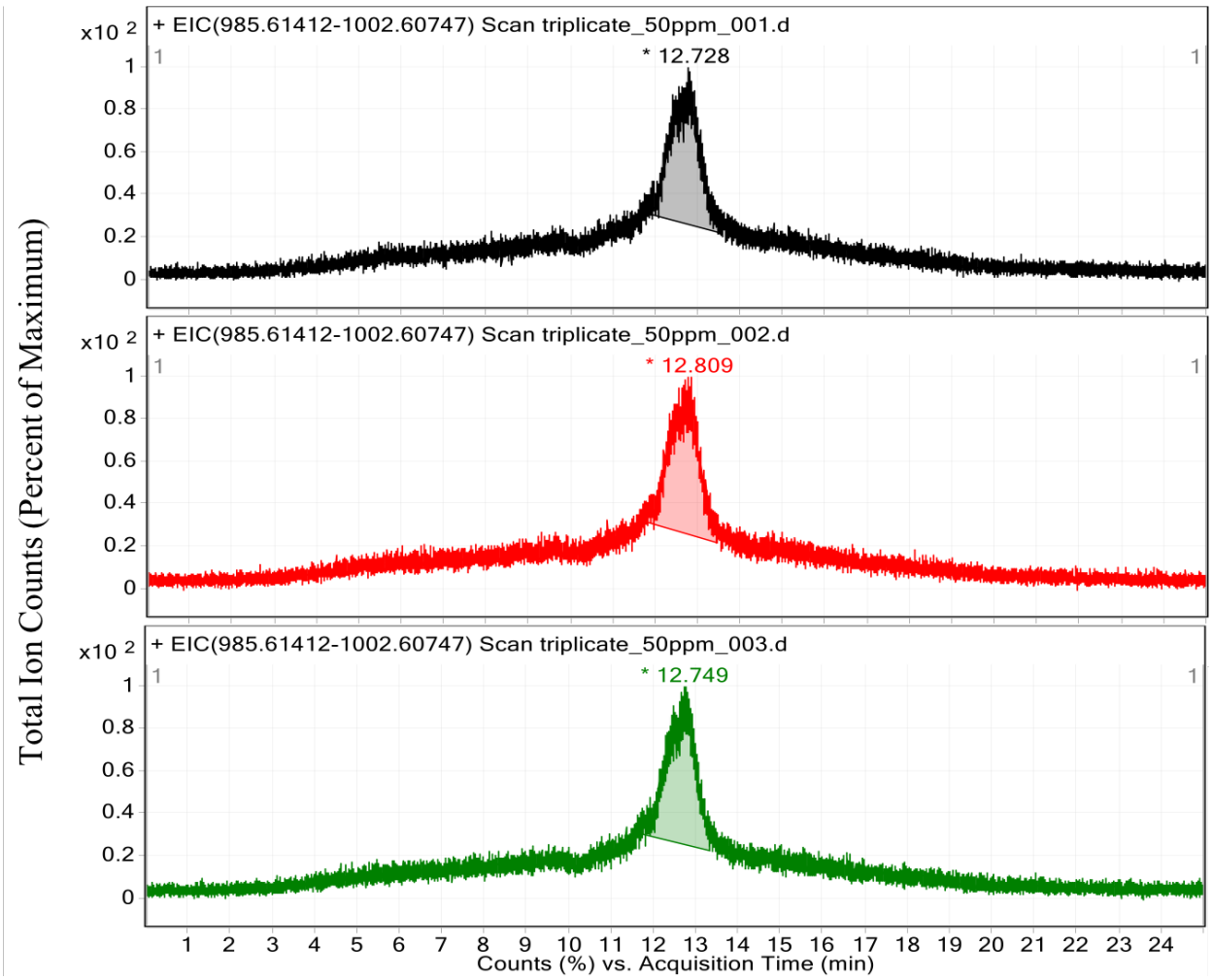

Figure 14. EIC spectrums of the triplicate runs of 50 ppm MCLR. The peak has been integrated and the peak retention time is listed above the peak. Peak integration was completed using standard peak parameters.

These integrated areas where then graphed against known concentration and fit with a linear regression.

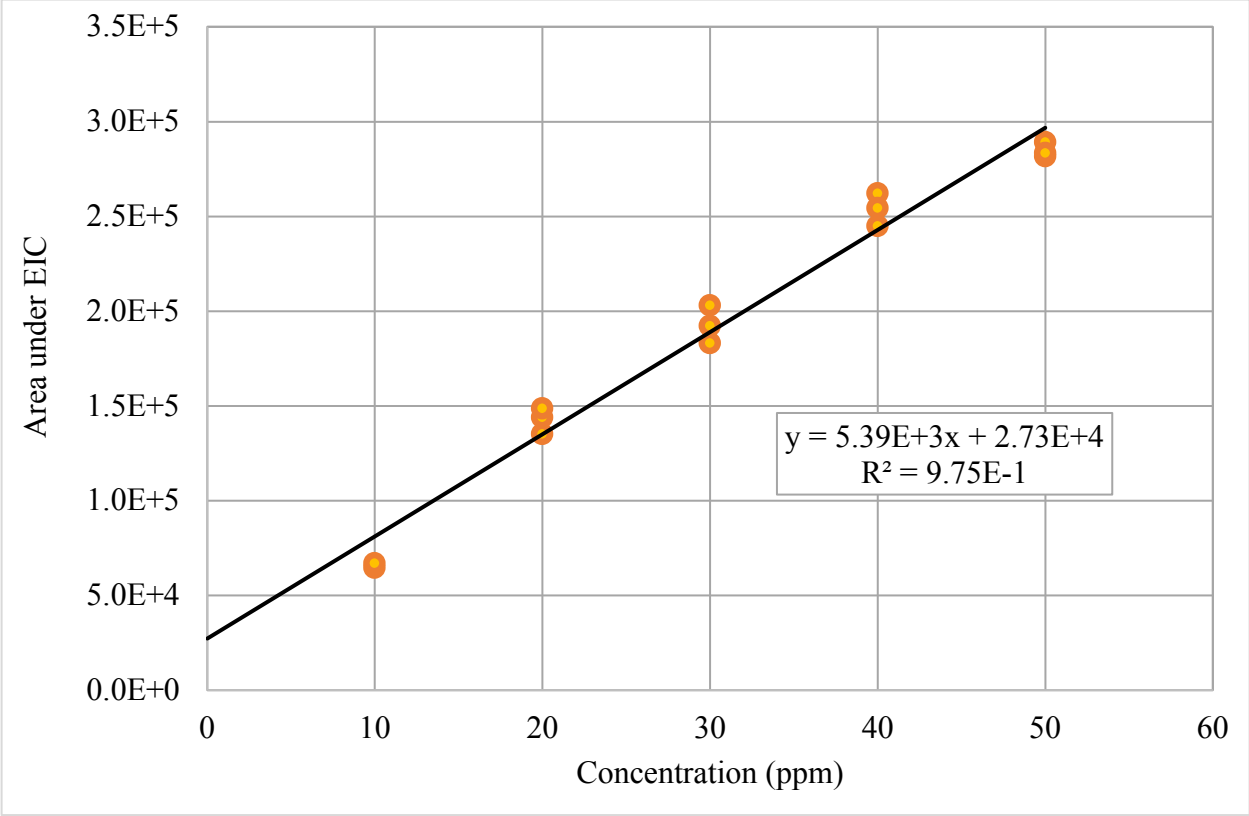

Figure 15. The triplicate MCLR serial dilutions, with a linear fit. The linear fit equation and R^2 value are displayed on the chart.

The limit of detection (LOD) based on three times the standard deviation of the regression line was 3.87 ppm.

The same process of gradient selection was then conducted for BMAA, with the TOF parameters remaining constant between the methods. Initially BMAA was run using the MCLR gradient, which was then refined to create the final gradient shown below.

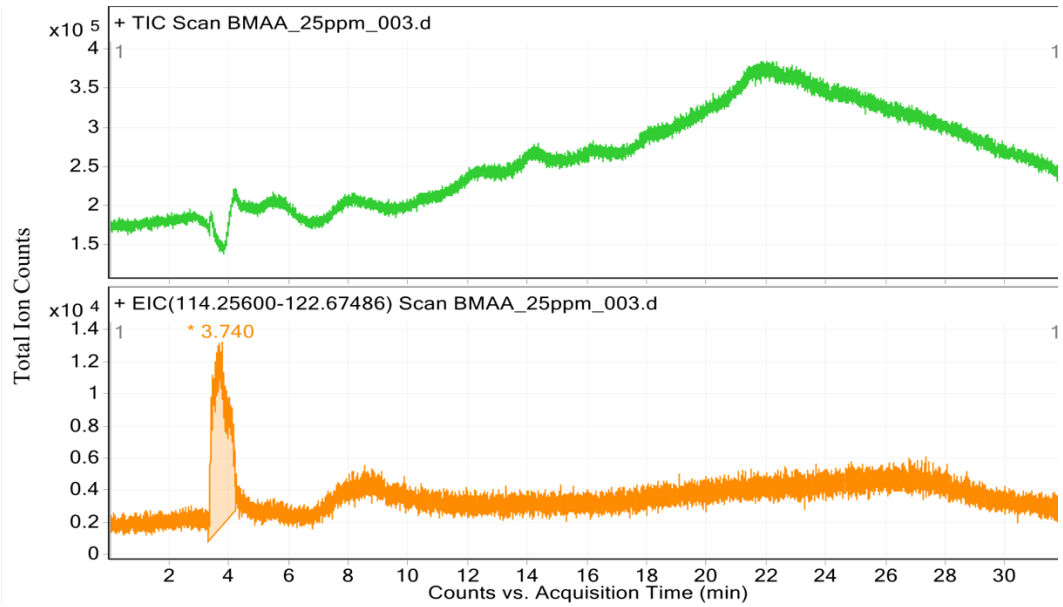

Figure 16. Total Ion Chromatograph (TIC) and Extracted Ion Chromatograph (EIC) of a 25 ppm BMAA standard run, with the final gradient used for the rest of the method.

The final gradient selected had a 3.7 minute retention time, and took 25 minutes for a complete run and is detailed in Appendix A. The EIC in Figure 16 show a singular BMAA peak which can be easily integrated. Again, the Mass Spectrum was used to confirm the identity of BMAA.

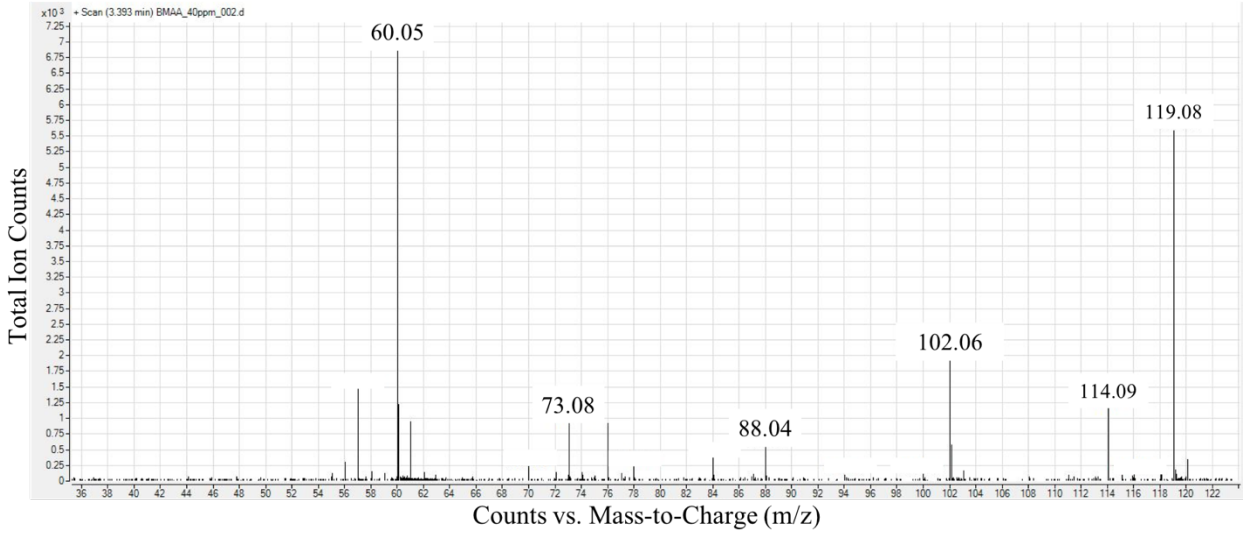

Figure 17. The full range mass spectrum at 3.93 minutes of a BMAA standard LCTOF run.

The above mass spectrum has a clear parent mass peak at 119.08 m/z, matching our desired mass peak. This mass is as given in Figure 6, plus one due to the positive ion being created for this method. Analyzing the isotope ratios further indicates this is the mass spectrum of BMAA. From Figure 6, the expected (+1) isotope ratio is 4.3%. In the above mass spectrum the calculated ratios is 5.2%. In addition, two fragments were

identified at 73.08 m/z and 102.06 m/z. The structures of these fragments are shown below.

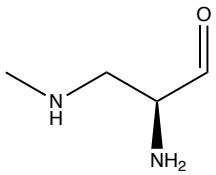

Chemical Formula: $C_4H_{10}N_2O$
Exact Mass: 102.08
Molecular Weight: 102.14
m/z: 102.08 (100.0%), 103.08 (4.3%)

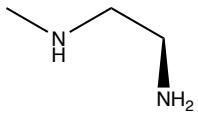

Chemical Formula: $C_3H_{10}N_2$
Exact Mass: 74.08
Molecular Weight: 74.13
m/z: 74.08 (100.0%), 75.09 (3.2%)
Elemental Analysis: C, 48.61; H, 13.60; N, 37.79

Figure 18. Above are the structures of the two BMAA fragments.

The mass spectrum was used to confirm the identity of MCLR for each run after this. With the gradient set, serial dilutions were prepared for BMAA and triplicate runs were done to create a BMAA calibration curve.

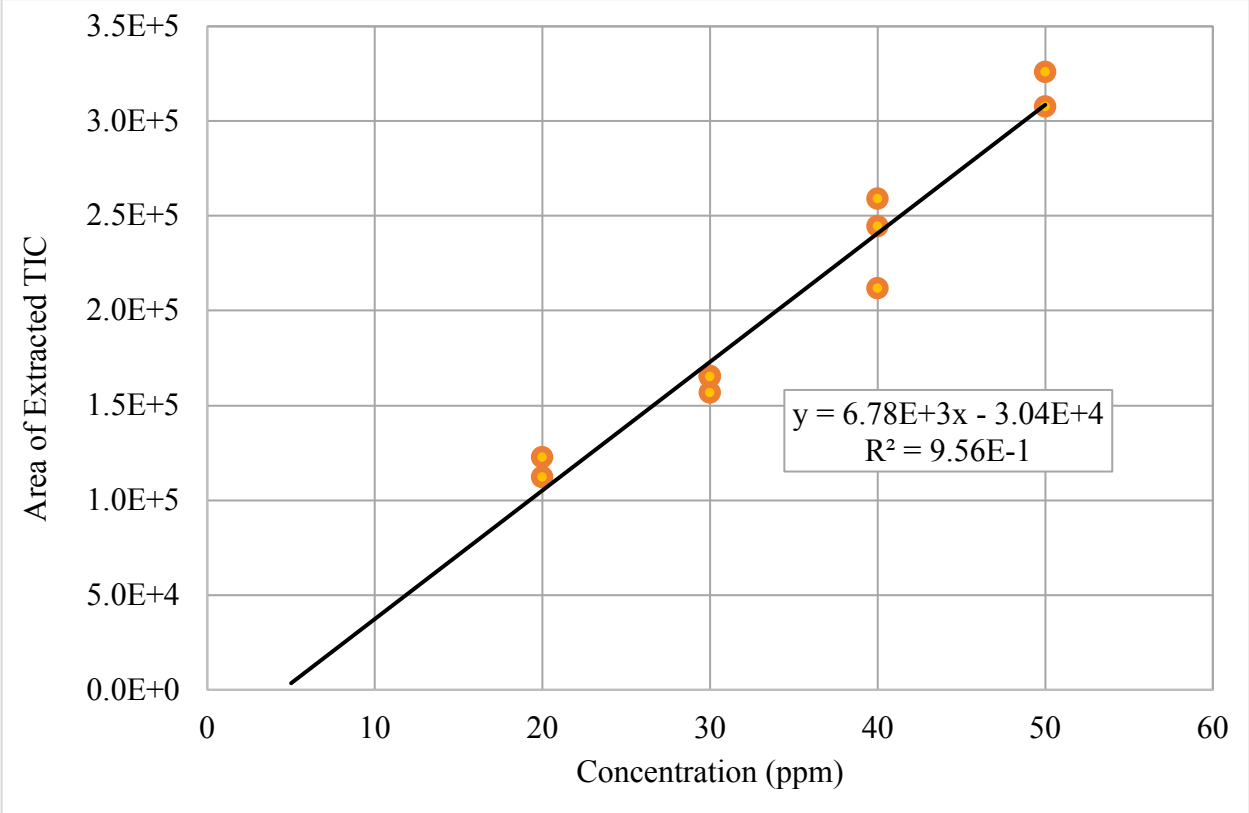

Figure 19. The triplicate BMAA serial dilutions, with a linear fit. The linear fit equation and R^2 value are displayed on the chart.

No values are displayed for the 10 ppm concentration because no peak was for in their respective EICs at 119 m/z. The LOD) based on three times the standard deviation of the regression line was 5.7 ppm.

ELISA

ELISA standards were run in triplicate in accordance with the manufacturers specifications. One run's data is graphed as is suggested by the manufacturers below. The quantitative range of this kit is 0.2 ppb to 2 ppb, as is apparent from the range of the calibration curve below. We only purchased the ELISA for MC, so this data analysis only corresponds to MC.

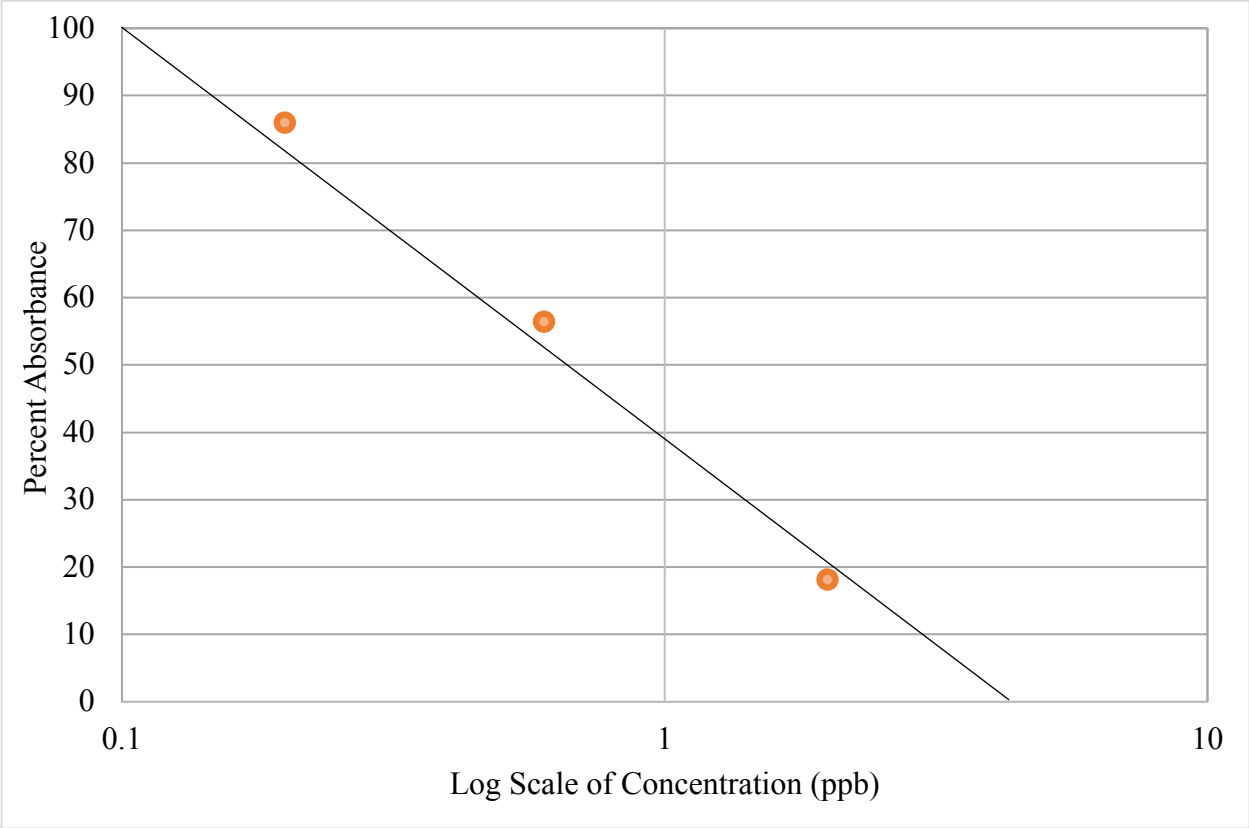

Figure 20. The MCLR standards graphed with a log scale on the concentration axis and a corresponding linear fit.

Discussion

HPLC/TOF MS

In the initial analysis of the MCLR standard (purchased from Thermo Fisher Scientific), it was noted that the MCLR was coming off in two distinct, base-line resolved peaks. This indicates that there are two conformations of MC within the sample. If the molecules were switching quickly between these conformations, they would come off as one peak, however the two peaks indicate that the change is slow enough to allow us to detect each in turn. Most likely this conformational difference has to do with the orientation of the peptide ring. The orientation difference is causing enough of a change in the chemical properties such that the molecules have a different affinity for the column. This isomerization was not seen in relative literature, which indicates it may have something to do with the specific standard used. While interesting, a main goal of

the gradient development was to make these distinct peaks overlap. Therefore, the intensity of the signal would be concentrated in one location, allowing one to more easily locate the corresponding EIC peak at low concentrations. The long initial retention times of 27 and 33 minutes was also undesirable and the gradients sought to shorten this time, without causing other peaks within the sample to overlap with that of MCLR. Ultimately this was successful and the final gradient used had one distinct peak, with a retention time of 12.7 minutes, as is seen in Figure 13. These results have a shorter column retention time than other similar analytical works (Barco, Rivera et al. 2002).

The MCLR triplicate data showed great agreement, leading to very small error values between the points. One thing to notice in Figure 15, is the potential slight curvature at 50 ppm, which could indicate the instrument is becoming over saturated at this concentration. To check this theory, the data was graphed again excluding the 50 ppm data set.

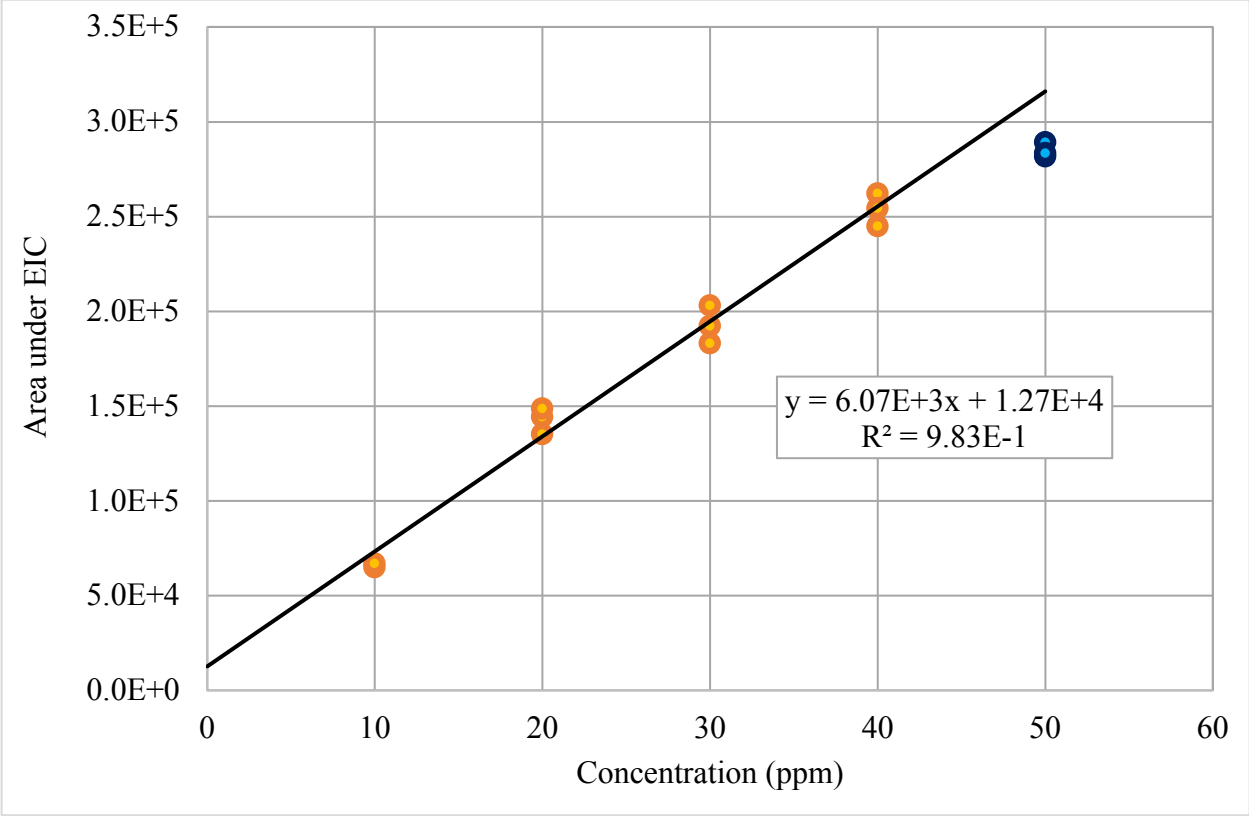

Figure 21. The triplicate MCLR serial dilutions. The 50ppm data points are displayed, but excluded from the linear fit. The linear fit equation and R^2 value are displayed on the chart.

In Figure 21 above, when the 50 ppm data points are excluded, the y-intercept approaches zero, and the R^2 value approaches 1. The y-intercept change agrees more with our anticipated intercept of zero. The R^2 value change further indicates that this is a better linear regression, supporting the hypothesis that there may be over concentration occurring at 50 ppm. Exclusion of these points changes the LOD from 3.9 to 3.4 ppm, which is a 10% improvement to our detection limit.

Based upon the WHO recreation limit of 2 ppb, and a much greater risk associated with 20 ppb (Organization 1999), it is clear that without pre-concentration

there will be no reading from the given calibration curve spanning 10 ppm to 50 ppm. Therefore the pre-concentration and extraction being prepared by Maddi Lavigne will be extremely important. Based on the data collected we will need a 1000 fold concentration in order to be within our detection limits. This will most likely be achieved by extracting 500 mL of lake water into 0.5mL of 70% methanol using an automated SPE system. This concentration is quite reasonable compared to other analytical papers which have required a 10,000 fold pre-concentration (Barco, Rivera et al. 2002).

The BMAA data collected indicates that the detection limits for BMAA will be less sensitive than that of MCLR, due to the lack of a signal at 10ppm and more variation in triplicate values. The presence of fragments in the mass spectrum could indicate that our analysis could benefit from a softer ionization, which could be achieved by lowering the capillary voltage value. The variation in triplicate values also indicates that it would be worthwhile to build a calibration curve with slightly greater concentration values. Due to the lack of data, it is difficult to know what concentration to expect during a bloom event on the Belgrades. However, with this data a concentrated sample can be prepared much like that of MC to determine what concentrations of BMAA are present in the Belgrades during bloom events.

ELISA

Although Envirologix (the manufacturers of the ELISA kit) suggest graphing calibration curve on a log scale, as is shown in Figure 20, this fails to show the sigmoidal nature of the curve. As discussed above, the kit is a competitive ELISA system, meaning that in accordance with Michaelis-Menten kinetics the relationship between absorbance and concentration will be sigmoidal.

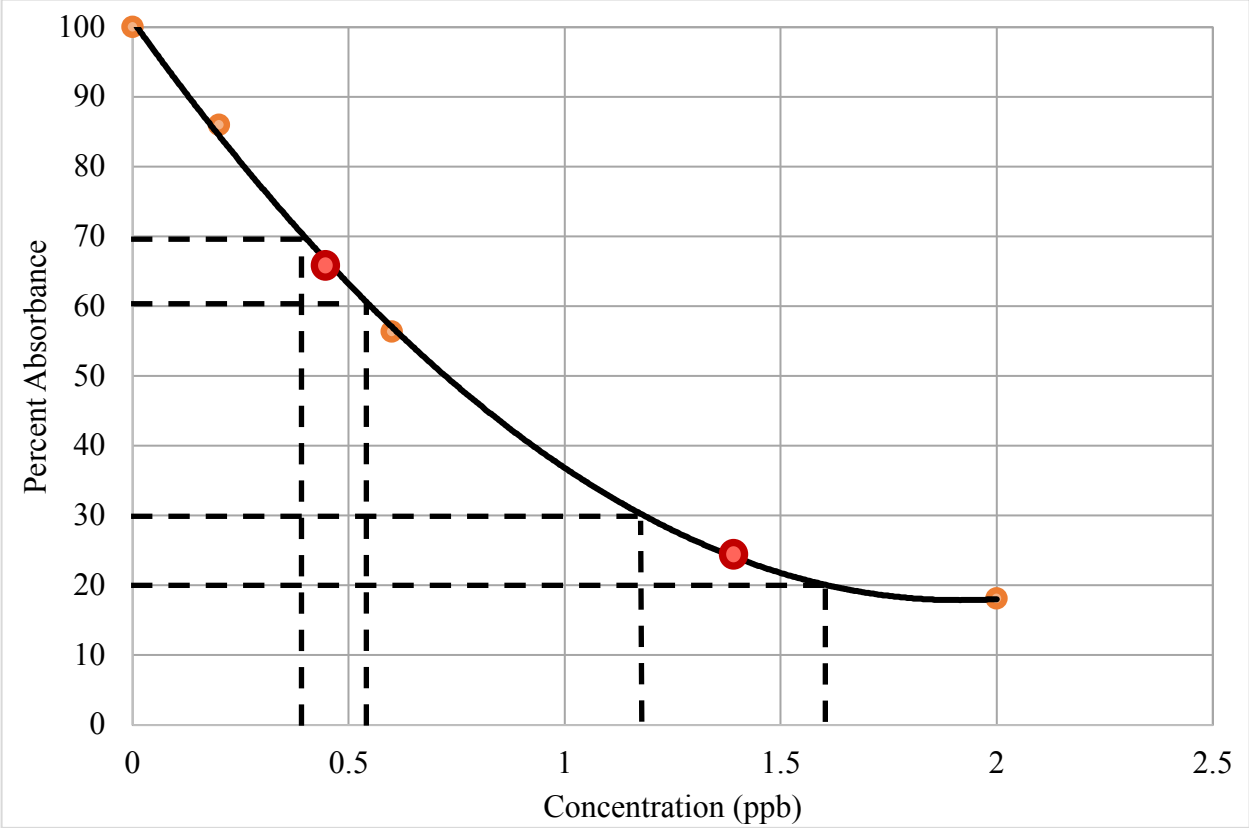

Figure 22. The MCLR standards graphed a sigmoidal fit. The two red points and corresponding doted lines pictorially demonstrate how the concentration error changes drastically over the ELISA detection range.

The fit in Figure 22 gives valuable information about how the kit works and how to interpret the data. We see that on the steep part of the curve, approximately 0.2 ppb to 1 ppb, with a given error in the absorbance value there is a relatively small error in concentration. However, as the concentration approaches 2 ppb, that error in concentration becomes greater. The linear fit seems to indicate that our data is equivalent anywhere on the calibration curve, whereas this fit demonstrates that as we approach 2 our error bars significantly increase. This further shows that at a reading of 2 ppb, the concentration is actually 2+, so it is known to be 2 or above but no information can be attained in regards to how much above 2 it is. This shows that while the ELISA kit may yield good data below the WHO limit of 2 ppb, it will not be helpful measuring MC as the concentrations exceed that limit. Calculating the LOD of the ELISA is more complicated due to the logarithmic dependence, as qualitatively discussed above. Between 0.2 and 1 ppb the calculate concentration range is ± 0.01 ppm, however between 1 ppb and 1.75 ppb, the calculated concentration range goes to ± 0.1 ppm. Therefore, it is clear that analytical uncertainties are dependent on the actual concentrations, and this must be kept in mind when using these kits for environmental sampling. Diluting samples with MCLR above 2 ppb is possible, but will double the analytical costs.

Conclusion and Future Directions

To determine how future research should proceed, we can directly compare the advantages and drawbacks of both analytical methods. ELISA kits for BMAA were not available at the time of this work, but have now become available. The new ELISA kits should be tested due to the recent recognition of the neurotoxic effects of BMAA. This work will compare ELISA and HPLC/TOF MS for MCLR alone. The first aspect is sample preparation. Samples must be pre-concentrated by a factor of 1000 before they can be run on the TOF given our current detection limits. The prospect of this extraction is made more manageable by the development of an automated concentration system currently being designed by another Colby student. In comparison, the ELISA kit can be run on water samples directly taken from the lake, removing a long and arduous step from the process. Ease of use of these instruments and processes is also a factor in future research directions. The ELISA kit is easier to operate, as it requires just the ability to pipette and the Spectra Max M5 is resoundingly straightforward to use. The TOF on the other hand requires knowledge of the instrument and the ability to trouble shoot. While it requires more training and chemical understanding, learning to operate the TOF system is incredibly rewarding as an undergraduate student and facilitates student learning as an integral part of the data collection process.

The time efficiency of running samples is a key factor designing an analytical method. On the ELISA system, one student can only run 16 samples in 90 minutes and must be present for the entire process as the timing is extremely important. On the TOF system, each method run is currently set up to take 24 minutes, however this could be cut down to 18 minutes without loss of accuracy. Most importantly the TOF has an autosampler, allowing one person to set up 100 samples at once. Then with enough solvent, the student need only return when all the runs are complete and extract the data. The additional of the autosampler, makes the LC/TOF a far more efficient data collection process. When the cost of associated instruments are excluded (LCTOF, M5 SpectraMax etc.), each samples costs $9 on the ELISA and only approximately $4 on the LC/TOF.

The last and most important factor is the molecular information provided by both systems. As was demonstrated with the TOF data, each mass spectrum can be analyzed to ensure that the extracted peak corresponds to the target molecule. The isotope ratios can be analyzed, along with the fragmentation pattern of these molecules. In comparison, the ELISA instructions are intentionally vague, such that no one can copy their product. Researchers have also found that some ELISA kits will give a MC reading for a severed Adda amino acid group (van Apeldoorn, van Egmond et al. 2007). As discussed above, a severed Adda amino acid has greatly reduced toxicity and could lead to a false positive reading of the ELISA kit. However, the same Adda amino acid would be produced as its own mass peak on the TOF and would allow one to determine the actual MC concentration. With all these factors considered, the TOF may require a more intense sample preparation, however it will contribute to many fewer false positive readings, and will continue to foster instrumental learning in undergraduate students at Colby. It would also be possible to use the two in conjunction, measure low level concentrations on the ELISA and higher concentrations on the TOF.

Moving forward this project will include a parameter optimization of the capillary voltage and source temperature, and the development of an automated SPE by Maddi

Lavigne. In addition to these analytical future steps, the development of a full analytical method will allow for microcystin and BMAA concertation data to be collected on the Belgrades during bloom events. Heading into the summer, samples from each of the Belgrades should be collected in the second week of August to be analyzed. Based on the concentration pre-factor, at least half a liter should be collected at each collection site. This should be done in the second week of August because this is generally when the most significant blue green blooms occur. Work done by Michaela Oberkfell last summer and other students previously has demonstrated that this second bloom has a much higher concentration of cyanobacteria than the first bloom. Samples should also be collected three days after the end of a bloom event, to see how the concentration changes as the cells lyse. The samples should first be analyzed on the ELISA kit, if the concentration is greater than 1.5 ppb, the sample should then be run on the LCTOF system. Using the two systems in conjunction will allow for the most efficient data processing. It would additionally be interesting to see if the concentrations of BMAA and MC covary. If that was the case it would allow one concentration to be estimated based on the other.

Acknowledgements

I would like to thank Prof. Whitney King for advising my Honors Thesis, Prof. Denise Bruesewitz for acting as my second reader, and the many students I have worked with this past year on the Belgrade lakes and in the lab. Additionally, I would like to thank the Colby Chemistry Department for funding this project and granting me unlimited time on the LC/TOF system.

Works Referenced

"LakeSmart." 2018, from https://mainelakessociety.org/lakesmart/.

(2018). QuantiPlate Kit for Microcystins, EnviroLogix.

Atia, A. and A. Saad (2014). Review on Freshwater Blue-Green Algae (Cyanobacteria): Occurrence, Classification and Toxicology.

Banack, S., T. Caller, P. Henegan, J. Haney, A. Murby, J. Metcalf, J. Powell, P. Cox and E. Stommel (2015). "Detection of Cyanotoxins, β-N-methylamino-L-alanine and Microcystins, from a Lake Surrounded by Cases of Amyotrophic Lateral Sclerosis." Toxins **7**(2): 322.

Banack, S. A., T. A. Caller and E. W. Stommel (2010). "The cyanobacteria derived toxin beta-N-methylamino-L-alanine and amyotrophic lateral sclerosis." Toxins **2**(12): 2837-2850.

Barco, M., J. Rivera and J. Caixach (2002). "Analysis of cyanobacterial hepatotoxins in water samples by microbore reversed-phase liquid chromatography–electrospray ionisation mass spectrometry." Journal of Chromatography A **959**(1): 103-111.

Beri, J., K. I. Kirkwood, D. C. Muddiman and M. S. Bereman (2018). "A novel integrated strategy for the detection and quantification of the neurotoxin β-N-methylamino-l-alanine in environmental samples." Analytical and Bioanalytical Chemistry **410**(10): 2597-2605.

Beusen, A. H. W., A. F. Bouwman, L. P. H. Van Beek, J. M. Mogollón and J. J. Middelburg (2016). "Global riverine N and P transport to ocean increased during the 20th century despite increased retention along the aquatic continuum." Biogeosciences **13**(8): 2441-2451.

Botes, D. P., H. Kruger and C. C. Viljoen (1982). "Isolation and characterization of four toxins from the blue-green alga, Microcystis aeruginosa." Toxicon **20**(6): 945-954.

Bradley, W. G. and D. C. Mash (2009). "Beyond Guam: The cyanobacteria/BMAA hypothesis of the cause of ALS and other neurodegenerative diseases." Amyotrophic Lateral Sclerosis **10**(SUPPL. 2): 7-20.

Caller, T., P. Henegan and E. Stommel (2018). "The Potential Role of BMAA in Neurodegeneration." Neurotoxicity Research **33**(1): 222-226.

Caller, T. A., J. W. Doolin, J. F. Haney, A. J. Murby, K. G. West, H. E. Farrar, A. Ball, B. T. Harris and E. W. Stommel (2009). "A cluster of amyotrophic lateral

sclerosis in New Hampshire: a possible role for toxic cyanobacteria blooms." Amyotroph Lateral Scler **10 Suppl 2**: 101-108.

Chasteen, T. G. (2003, 2005, 2006). "CZE, CITP and CIEF: Modes of Capillary Electrophoresis." Retrieved 11/4/2018, 2018, from http://www.shsu.edu/~chm_tgc/primers/pdf/CEs.pdf.

Cox, P. A., S. A. Banack and S. J. Murch (2003). "Biomagnification of cyanobacterial neurotoxins and neurodegenerative disease among the Chamorro people of Guam." Proc Natl Acad Sci U S A **100**(23): 13380-13383.

Cox, P. A., S. A. Banack, S. J. Murch, U. Rasmussen, G. Tien, R. R. Bidigare, J. S. Metcalf, L. F. Morrison, G. A. Codd and B. Bergman (2005). "Diverse taxa of cyanobacteria produce β-N-methylamino-L-alanine, a neurotoxic amino acid." Proceedings of the National Academy of Sciences of the United States of America **102**(14): 5074-5078.

Dawson, R. M. (1998). "The toxicology of microcystins." Toxicon **36**(7): 953-962.

de Munck, E., E. Munoz-Saez, M. T. Antonio, J. Pineda, A. Herrera, B. G. Miguel and R. M. Arahuetes (2013). "Effect of beta-N-methylamino-L-alanine on oxidative stress of liver and kidney in rat." Environ Toxicol Pharmacol **35**(2): 193-199.

Dittmann, E. and C. Wiegand (2006). "Cyanobacterial toxins - Occurrence, biosynthesis and impact on human affairs." Molecular Nutrition and Food Research **50**(1): 7-17.

EPA (2016). Human Health Recreational Ambient Water Quality Criteria or Swimming Advisories for Microcystins and Cylindrospermopsin.

Fawell, J. K., R. E. Mitchell, D. J. Everett and R. E. Hill (1999). "The toxicity of cyanobacterial toxins in the mouse: I microcystin-LR." Hum Exp Toxicol **18**(3): 162-167.

Fontanillo, M. and M. Köhn (2018). "Microcystins: Synthesis and structure–activity relationship studies toward PP1 and PP2A." Bioorganic & Medicinal Chemistry **26**(6): 1118-1126.

Funari, E. and E. Testai (2008). "Human Health Risk Assessment Related to Cyanotoxins Exposure." Critical Reviews in Toxicology **38**(2): 97-125.

Holtcamp, W. (2012). "The Emerging Science of BMAA: Do Cyanobacteria Contribute to Neurodegenerative Disease?" Environmental Health Perspectives **120**(3): a110-a116.

Huisman, J., G. A. Codd, H. W. Paerl, B. W. Ibelings, J. M. H. Verspagen and P. M.

Visser (2018). "Cyanobacterial blooms." Nature Reviews Microbiology **16**(8): 471-483.

Le Moal, M., C. Gascuel-Odoux, A. Ménesguen, Y. Souchon, C. Étrillard, A. Levain, F. Moatar, A. Pannard, P. Souchu, A. Lefebvre and G. Pinay (2019). "Eutrophication: A new wine in an old bottle?" Science of The Total Environment **651**: 1-11.

Lequin, R. M. (2005). "Enzyme immunoassay (EIA)/enzyme-linked immunosorbent assay (ELISA)." Clin Chem **51**(12): 2415-2418.

Lipton, S. A. (2004). "Failures and Successes of NMDA Receptor Antagonists: Molecular Basis for the Use of Open-Channel Blockers like Memantine in the Treatment of Acute and Chronic Neurologic Insults." NeuroRx **1**(1): 101-110.

Lobner, D., P. M. T. Piana, A. K. Salous and R. W. Peoples (2007). "β-N-methylamino-l-alanine enhances neurotoxicity through multiple mechanisms." Neurobiology of Disease **25**(2): 360-366.

Ma, J., Y. Li, M. Wu and X. Li (2018). "Oxidative stress-mediated p53/p21WAF1/CIP1 pathway may be involved in microcystin-LR-induced cytotoxicity in HepG2 cells." Chemosphere **194**: 773-783.

MacKintosh, C., K. A. Beattie, S. Klumpp, P. Cohen and G. A. Codd (1990). "Cyanobacterial microcystin-LR is a potent and specific inhibitor of protein phosphatases 1 and 2A from both mammals and higher plants." FEBS Letters **264**(2): 187-192.

Marino, M. J., O. Valenti and P. J. Conn (2003). "Glutamate receptors and Parkinson's disease: Opportunities for intervention." Drugs and Aging **20**(5): 377-397.

Merel, S., D. Walker, R. Chicana, S. Snyder, E. Baurès and O. Thomas (2013). "State of knowledge and concerns on cyanobacterial blooms and cyanotoxins." Environment International **59**: 303-327.

Murch, S. J., P. A. Cox and S. A. Banack (2004). "A mechanism for slow release of biomagnified cyanobacterial neurotoxins and neurodegenerative disease in Guam." Proceedings of the National Academy of Sciences of the United States of America **101**(33): 12228.

World Health Organization (1999). Toxic Cyanobacteria in Water: A guide to their public health consequences, monitoring and management. I. C. a. J. Bartam. London and New York, WHO.

Orr, P. T. and G. J. Jones (1998). "Relationship between microcystin production and cell division rates in nitrogen-limited Microcystis aeruginosa cultures." Limnology

and Oceanography **43**(7): 1604-1614.

Paerl, H. W. and J. Huisman (2008). "Blooms Like It Hot." Science **320**(5872): 57.

Pinay, G., S. Peiffer, J. R. De Dreuzy, S. Krause, D. M. Hannah, J. H. Fleckenstein, M. Sebilo, K. Bishop and L. Hubert-Moy (2015). "Upscaling Nitrogen Removal Capacity from Local Hotspots to Low Stream Orders' Drainage Basins." Ecosystems **18**(6): 1101-1120.

Ramya, M., M. Kayalvizhi, G. Haripriya and P. Rathinasabapathi (2018). "Detection of microcystin-producing cyanobacteria in water samples using loop-mediated isothermal amplification targeting mcyB gene." 3 Biotech **8**(9).

Robinson, N. A., J. G. Pace, C. F. Matson, G. A. Miura and W. B. Lawrence (1991). "Tissue distribution, excretion and hepatic biotransformation of microcystin-LR in mice." Journal of Pharmacology and Experimental Therapeutics **256**(1): 176-182.

Rodgers, K. J., B. J. Main and K. Samardzic (2018). "Cyanobacterial Neurotoxins: Their Occurrence and Mechanisms of Toxicity." Neurotoxicity Research **33**(1): 168-177

Sarazin, G., C. Quiblier-Llobéras, G. Bertru, L. Brient, C. Vezie, C. Bernard, A. Couté, M. C. Hennion, C. Robillot and N. Tandeau de Marsac (2002). "First assessment of the toxical risk associated with fresh water cyanobacteria in France: The "EFFLOCYA" research program." Revue des Sciences de l'Eau **15**(1): 315-326.

Shi, L., W. W. Carmichael and P. J. Kennelly (1999). "Cyanobacterial PPP family protein phosphatases possess multifunctional capabilities and are resistant to microcystin-LR." Journal of Biological Chemistry **274**(15): 10039-10046.

Stommel, E. W., N. C. Field and T. A. Caller (2013). "Aerosolization of cyanobacteria as a risk factor for amyotrophic lateral sclerosis." Medical Hypotheses **80**(2): 142-145.

van Apeldoorn, M. E., H. P. van Egmond, G. J. Speijers and G. J. Bakker (2007). "Toxins of cyanobacteria." Mol Nutr Food Res **51**(1): 7-60.

Yung, S. C., Y. Zhou, C. M. Irvin, B. Kirkpatrick and L. C. Backer (2007). "Characterization of aerosols containing microcystin." Marine Drugs **5**(4): 136-150.

Zhang, D., P. Xie, Y. Liu and T. Qiu (2009). "Transfer, distribution and bioaccumulation of microcystins in the aquatic food web in Lake Taihu, China, with potential risks to human health." Science of The Total Environment **407**(7): 2191-2199.

Appendix A: LC-MS Gradient Details

Table 3. Final gradient used for MC HPLC runs.

Time	Acetonitrile (%)	Water (%)	Flow Rate (ml/min)	Maximum Pressure (Bar)
0	10	90	0.200	400
4	20	80	0.200	400
8	25	75	0.200	400
10	30	70	0.200	400
15	20	80	0.200	400
20	10	90	0.200	400
25	10	90	0.200	400

Apendix B: Envirologix ELISA Manual

ENVIROLOGIX™

QuantiPlate™ Kit for Microcystins

Highlights:

- *Quantitative laboratory detection of Microcystin toxin in surface water*
- *Detects from 0.2 to 2.0 ppb*

Contents of Kit:

- *12 strips of 8 antibody-coated wells each, in plate frame*
- *1 vial of Negative Control*
- *1 vial of 0.2 ppb Microcystin LR Calibrator*
- *1 vial of 0.6 ppb Microcystin LR Calibrator*
- *1 vial of 2.0 ppb Microcystin LR Calibrator*
- *1 bottle of Assay Diluent*
- *1 bottle of Microcystin-enzyme Conjugate*
- *1 packet of Wash Solution salts*
- *1 bottle of Substrate*
- *1 bottle of Stop Solution*

Precision

	Recovery (%CV)	OD (%CV)
Intra-Assay		**n=11**
0.4 ppb	8.3%	4.1%
1.0 ppb	4.6%	5.9%
Inter-Assay		**n=11**
0.4 ppb	8.7%	8.7
1.0 ppb	3.6%	11.7

Cross-Reactivity

Compound	50% B_0	LOD 80% B_0
Microcystin LR	0.53	0.21
Microcystin LA	0.91	0.16
Microcystin RR	0.69	0.27
Microcystin YR	0.84	0.36
Nodularin	0.30	0.12

Catalog Number EP 022

Intended Use

The EnviroLogix QuantiPlate Kit for Microcystins is designed for the quantitative laboratory detection of Microcystin toxin in surface water samples, with an assay quantitation range from 0.2 to 2 parts per billion (ppb)

How the Test Works

This QuantiPlate Kit for Microcystins is a competitive Enzyme-Linked ImmunoSorbent Assay (ELISA).

In the test, Microcystin toxin in the sample competes with enzyme (horseradish peroxidase)-labeled Microcystin for a limited number of antibody binding sites on the inside surface of the test wells.

After a simple wash step, the outcome of the competition is visualized with a color development step. As with all competitive immunoassays, sample concentration is inversely proportional to color development.

Darker color = Lower concentration
Lighter color = Higher concentration

Limit of Detection

The Limit of Detection (LOD) of this Kit is 0.10 ppb. The LOD was determined by interpolation at 91.6% B_0* from a standard curve. 91.6% B_0 was determined to be 3 standard deviations from the mean of a population of negative water samples.

*100% B_0 equals the maximum amount of Microcystin-enzyme conjugate that is bound by the antibody in the absence of any Microcystin in the sample (i.e. negative control). $\%B_0$ = (OD of Sample or Calibrator/OD of Negative Control) x 100.

Limit of Quantification

The Limit of Quantification (LOQ) of this Kit was validated at 0.2 ppb. The LOQ was determined by fortifying a population of negative water samples at 0.2 ppb. The mean recovery was 96.4% with a coefficient of variation (CV) [(standard deviation/mean) x 100] of 8.2%.

Precision

Microcystin-fortified control solutions were repetitively analyzed both within a single assay, and in different assays on different days. The data is expressed as %CV for both the recovered concentration and for absorbance (OD).

Fortification and Recovery

Four surface water samples were fortified with Microcystin to a concentration of 1.0 ppb. The average recovery was 102%, with a CV of 4.2%.

Cross-Reactivity

This Kit does not distinguish between the Microcystin toxin variants, but detects their presence to differing degrees. The accompanying table shows the value for 50% B_0 and the value for the 80% B_0 for four Microcystin toxin variants and nodularin toxin. Concentration is in ppb. Humic acid did not interfere in the assay up to a concentration of 100 ppm.

Rev. 04-22-16


Remove unneeded strips


Select Calibrators and Control

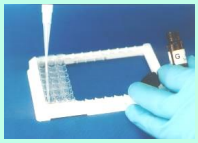
Add controls/calibrators/sample

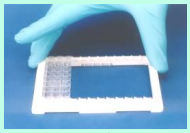
Mix plate


Incubate


Bottle Wash method

Materials Needed

- disposable tip adjustable air-displacement pipette which will measure 50 µL and 100 µL
- marking pen (indelible)
- tape or Parafilm®
- timer (30 minutes)
- distilled water for preparing Wash Solution
- glassware for storing Wash Solution
- wash bottle for washing strips with Wash Solution
- microtiter plate reader or strip reader
- microtiter plate washer (optional)
- twelve or 8-channel pipette that will measure 50 µL and 100 µL (optional)
- racked (glass) dilution tubes for loading samples into the plate with a 12-channel pipette (optional)
- orbital plate shaker (optional)

Preparation of Solutions

Wash Buffer:
To make 1 L, add the contents of one packet of phosphate-buffered saline - Tween 20, pH 7.4 (**Wash Solution salts**) to 1 L of distilled water. Mix thoroughly to dissolve the salts. This can be stored at room temperature.

How to Run the Assay

- Read all of these instructions before running the kit.
- Allow all reagents to reach room temperature before beginning (at least 30 minutes with un-boxed strips and reagents at room temperature - do not remove strips from bag with desiccant until they have warmed up).
- Organize all samples, reagents and pipettes so that steps 1 and 2 can be performed in 10 minutes or less.
- If more than three strips are to be run at one time, the 10 minutes is likely to be exceeded, and the use of a multi-channel pipette is recommended (see "Note" below).
- If three or fewer strips are to be run, use a disposable-tip air-displacement pipette and a clean pipette tip to add each Calibrator and sample to the wells. Assay Diluent, Conjugate, Substrate, and Stop Solution may be added in the same manner; alternatively, use a repeating pipette with a disposable tip on the end of the Combitip for these three reagents.
- If fewer than all twelve strips are used, reseal the unneeded strips and the desiccant in the plastic bag provided.
- Use the well identification markings on the plate frame to guide you when adding the samples and reagents. Two strips may be used to run the Negative Control (NC), three Calibrators (C1-C3) and four samples, in duplicate. More samples require more strips. For an example plate layout see Figure 1.

1. Rapidly add **50 µL** of **Microcystin Assay Diluent** to each well that will be used, preferably with a repeating or multi-channel pipetter.
2. Immediately add **50 µL** of **Negative Control** (NC), **50 µL** of each **Calibrator** (C1-C3) and **50 µL** of each **sample** (S1-S8) to their respective wells, as shown at left. (Follow this same order of addition for all reagents.) **Do not add Microcystin-enzyme Conjugate in this step.**

Strip Plate Wash option

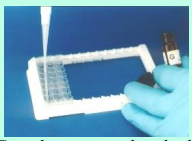

Complete protocol and add Stop Solution

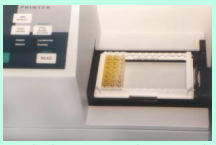

Read plates in a Plate Reader within 30 minutes of the addition of Stop Solution

Illustrative standard curve

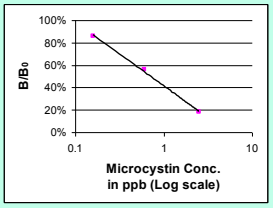

3. Thoroughly mix the contents of the wells by moving the strip holder in a rapid circular motion on the benchtop for a full 20-30 seconds. Be careful not to spill the contents!

NOTE: In order to minimize setup time it is recommended that a multi-channel pipette be used in steps 1, 2, 5, 8 and 10 when more than 3 strips are used.

4. Cover the wells with tape or Parafilm to prevent evaporation and incubate at ambient temperature for 30 minutes. If an orbital shaker is available shake at 200 rpm.
5. Add **50 µL** of **Microcystin-enzyme Conjugate** to each well. Do not empty the well contents or wash the strips at this time.
6. Thoroughly mix the contents of the wells as in step 3. Cover the wells with tape or Parafilm and incubate at ambient temperature for 30 minutes. Use orbital shaker if available.
7. After incubation, carefully remove the covering and vigorously shake the contents of the wells into a sink or other suitable container. Flood the wells completely with **Wash Solution**, then shake to empty. Repeat this wash step four times. Slap the plate on a paper towel to remove as much Wash Solution as possible. Alternatively, use a microtiter plate washer with **Wash Solution** for the wash step.
8. Add **100 µL** of **Substrate** to each well.
9. Thoroughly mix the contents of the wells, as in step 3. Cover the wells with new tape or Parafilm and incubate for 30 minutes at ambient temperature. Use orbital shaker if available.

Caution: Stop Solution is 1.0 N Hydrochloric acid. Handle carefully.

10. Add **100 µL** of **Stop Solution** to each well and mix thoroughly. This will turn the well contents yellow.

NOTE: Read the plate within 30 minutes of the addition of Stop Solution.

How to Interpret the Results

Spectrophotometric Measurement

1. Set the wavelength of your microtiter plate reader to 450 nanometers (nm). (If it has dual wavelength capability, use 600, 630 or 650 nm as the reference wavelength.)
2. If the plate reader does not auto-zero on air, zero the instrument against 200 µL water in a blank well. Measure and record the optical density (OD) of each well's contents. Alternatively, measure and record the OD in every well, then subtract the OD of the water blank from each of the readings.
3. A semi-log curve fit should be used for the standard curve if the microtiter plate reader you are using has data reduction capabilities. If not, calculate the results manually as described in the next section.

How to Calculate the Quantitative Results

1. After reading the wells, average the OD of each set of calibrators and samples, and calculate the $\%B_0$ as follows:

$$\%B_0 = \frac{\text{average OD of Calibrator or sample}}{\text{average OD of Negative Control}} \times 100$$

Precautions and Notes

- *Store all components at 4°-8°C (39°-46°F) when not in use.*
- *Do not expose components to temperatures greater than 37°C (99°F) or less than 2°C (36°F).*
- *Allow all reagents to reach ambient temperature (18°C to 27°C or 64°F to 81°F) before use.*
- *Do not use kit components after the expiration date.*
- *Do not use reagents or test well strips from one QuantiPlate Kit with reagents or test well strips from a different QuantiPlate Kit.*
- *Do not expose **Substrate** to **sunlight** during pipetting or while incubating in the test wells.*
- *Do not dilute or adulterate test reagents or use samples not called for in the test procedure.*
- *As with all tests, it is recommended that results be confirmed by an alternate method when necessary.*
- *Observe any applicable regulations when disposing of samples and kit reagents.*
- *Microcystin LR in aqueous solution will stick to plastics such as polypropylene. Collect and process samples in glass containers. Clear samples free of organic material can be stored refrigerated for up to two weeks before analysis.*

The $\%B_0$ calculation is used to equalize different runs of an assay. While the raw OD values of Negative Controls, Calibrators, and samples may differ from run to run, the $\%B_0$ relationship of calibrators and samples to the Negative Control should remain fairly constant.

The CV for each pair of Calibrator and sample OD values should not exceed 15%.

2. Graph the $\%B_0$ of each Calibrator against its Microcystin concentration on a semi-log scale (see Illustrative Standard Curve, left).
3. Determine the Microcystin concentration of each sample by finding its $\%B_0$ value and the corresponding concentration level on the graph.
4. Interpolation of sample concentration is only possible if the $\%B_0$ of the sample falls within the range of $\%B_0$'s of the Calibrators.

If the $\%B_0$ of a sample is higher than that of the lowest Calibrator, the sample must be reported as less than 0.2 ppb.

If the $\%B_0$ of a sample is lower than that of the highest Calibrator, the sample must be reported as greater than 2.0 ppb. If a concentration must be determined for these high level samples, dilute the sample 1:8 in distilled water. Run this dilution in a repeat of the immunoassay. If the result now falls within the range of the $\%B_0$'s of the Calibrators, you must then multiply the concentration measured in the diluted sample by a factor of 8.

Figure 1a. Example of a typical plate setup. (1 x 8 strips)

	1	2	3	4	5	6	7	8	9	10	11	12
A	NC	NC										
B	C1	C1										
C	C2	C2										
D	C3	C3										
E	S1	S1										
F	S2	S2										
G	S3	S3										
H	S4	S4										

Figure 2a. Illustrative quantitative calculations

Well contents	OD	Average OD	%CV	$\%B_0$	Microcystin Concentration (ppb)
Negative Control	1.398 1.347	1.373	2.628	100	NA
0.2ppb Calibrator	1.184 1.177	1.181	0.419	86	NA
0.6 ppb Calibrator	0.773 0.776	0.775	0.274	56.4	NA
2.0 ppb Calibrator	0.246 0.250	0.248	1.14	18.1	NA
Sample	0.573 0.567	0.570	0.744	41.5	1.01

**Actual values may vary; this data is for demonstration purposes only.*